ScienceImmunology

Submitted Manuscript: Confidential template updated: July 5 2016

The non-canonical inflammasome provides host defense via gasdermin D-dependent neutrophil extracellular traps

Authors: Kaiwen W. Chen[1,2*], Mercedes Monteleone[1*], Dave Boucher[1*], Gabriel Sollberger[3], Divya Ramnath[1], Nicholas D. Condon[1], Jessica B. von Pein[1], Petr Broz[2], Matthew J. Sweet[1], Kate Schroder[1]†

Affiliations:

[1]Institute for Molecular Bioscience (IMB), and IMB Centre for Inflammation and Disease Research, The University of Queensland, St Lucia Brisbane 4072, Australia.

[2]Department of Biochemistry, University of Lausanne, CH-1066 Epalinges, Switzerland.

[3]Max Planck Institute for Infection Biology, Department of Cellular Microbiology, Charitéplatz 1, Berlin

*These authors contributed equally

†Corresponding author: Dr. Kate Schroder, Institute for Molecular Bioscience (IMB), and IMB Centre for Inflammation and Disease Research, The University of Queensland, St Lucia 4072, Australia. Tel: +61 7 3346 2058, Fax: +61 7 3346 2101, E-mail: K.Schroder@imb.uq.edu.au

One Sentence Summary: Neutrophils defend against cytosolic bacteria by extruding neutrophil extracellular traps via the pore-forming protein, gasdermin D.

Abstract

Neutrophil extrusion of neutrophil extracellular traps (NETs) and concomitant cell death (NETosis) provides host defense against extracellular pathogens, while macrophage death by pyroptosis enables defense against intracellular pathogens. Here we report the surprising discovery that gasdermin D (GSDMD) connects these cell death modalities. We show that neutrophil exposure to cytosolic lipopolysaccharide or cytosolic Gram-negative bacteria (*Salmonella ΔsifA*, *C. rodentium*) activates non-canonical (caspase-4/11) inflammasome signaling and triggers GSDMD-dependent neutrophil death. Remarkably, GSDMD-dependent death induces neutrophils to extrude antimicrobial NETs. Caspase-11 and GSDMD are required for neutrophil plasma membrane rupture during the final stage of NET extrusion. Unexpectedly, caspase-11 and GSDMD are also required for early features of NETosis, including nuclear delobulation and DNA expansion; this is mediated by the coordinate actions of caspase-11 and GSDMD in mediating nuclear membrane permeabilization and histone degradation. *In vivo* application of DNase I to dissolve NETs during murine *Salmonella ΔsifA* challenge increases bacterial burden in wild-type but not *Casp11*$^{-/-}$ and *Gsdmd*$^{-/-}$ mice. Our studies reveal that neutrophils employ an inflammasome- and GSDMD-dependent mechanism to activate NETosis as a defense response against cytosolic bacteria.

Introduction

Newly described forms of non-apoptotic, programmed cell death in myeloid cells are emerging as critical drivers of both inflammatory pathologies and host defense. Inflammatory cell lysis by pyroptosis is extensively characterized in macrophages (*1, 2*), while neutrophils can die by expelling neutrophil extracellular traps (NETs) (*3*). Pyroptosis is initiated by inflammasome-activated inflammatory caspases (e.g. caspase-1, -4, -5, -11), which cleave Gasdermin D (GSDMD) to trigger plasma membrane pores (*1, 2, 4-8*). For example in macrophages, active caspase-1 cleaves GSDMD to elicit GSDMD-p30 pores and drive pyroptosis during signaling by canonical inflammasomes, such as those assembled by nod-like receptor (NLR) pyrin domain-containing 3 (NLRP3) and NLR CARD domain-containing 4 (NLRC4) (*1, 2, 8*). Macrophage

pyroptosis can also be triggered by the non-canonical inflammasome, which confers host defense against Gram-negative bacteria in the cytosol. In this pathway, murine caspase-11 or human caspase-4/5 directly recognize cytosolic bacterial lipopolysaccharide (LPS) from Gram-negative bacteria, triggering caspase-4/5/11 activation, GSDMD cleavage, GSDMD-p30 plasma membrane pores, NLRP3 signaling and cell lysis (*1, 2, 4, 9-12*). Macrophage pyroptosis is an important innate immune defense mechanism, as it exposes vacuole- and cytosol-resident pathogens to neutrophil-mediated extracellular destruction (*13, 14*). We, and others, previously reported that active caspase-1 does not trigger pyroptosis in neutrophils (*15-17*), suggesting that GSDMD is unable to elicit neutrophil cell death in this context. The ability of neutrophils to resist caspase-1-directed pyroptosis allows these cells the lifespan to perform their classic antimicrobial functions (degranulation, generation of reactive oxygen species) to kill the pathogen at a site of infection (*15*). The capacity of neutrophils to signal via the non-canonical inflammasome is unknown.

Under specific conditions, neutrophils can also neutralize extracellular pathogens via a non-classical mechanism, in which neutrophils expel NETs, web-like structures of DNA embedded with anti-microbial proteins, which ensnare and neutralize microbes (*3*). Neutrophil death by NET extrusion (NETosis) is a multi-stage process, involving first disintegration of the nuclear envelope and granule membranes and chromatin relaxation, leading to nuclear delobulation and DNA expansion within the intact cell. During this early stage of NETosis, proteins such as myeloperoxidase (MPO) and neutrophil elastase (NE) that normally reside in granules, mix with the DNA (*18*). Chromatin relaxation is mediated by histone inactivation, for example by protein arginine deiminase-4 (PAD4)-dependent histone citrullination (*19, 20*), or by histone degradation by the granule protease NE (*18*). In the final stage of NETosis, the plasma membrane ruptures, leading to the extrusion of DNA from the neutrophil. The signaling mechanisms underlying NETosis are only partially characterized (*21*).

Here, we investigated the capacity of neutrophils to undergo cell death downstream of canonical and non-canonical inflammasomes. Although neutrophils are resistant to cell death downstream of canonical inflammasomes, we found that non-canonical inflammasome signaling triggered

GSDMD-induced cell death and the extrusion of host-protective NETs. Our data thus reveal an unexpected mechanism of neutrophil-mediated host defense against cytosolic intruders.

Results

Neutrophils resist caspase-1-mediated pyroptosis but are sensitive to caspase-11-driven death

We previously reported that canonical inflammasome activation in neutrophils triggered caspase-1 activation and the secretion of mature interleukin (IL)-1β but not pyroptosis (*15*). To investigate the mechanisms by which neutrophils resist caspase-1-driven pyroptosis, we performed parallel assays in bone marrow-derived macrophages and mature bone marrow neutrophils from wild-type (WT) versus *Gsdmd*-deficient mice. We used a well-established protocol to activate caspase-1, in which cells are primed with a toll-like receptor (TLR) ligand (e.g. lipopolysaccharide, LPS) to upregulate the expression of the inflammasome sensor and pro-IL-1β, before challenge with log phase *Salmonella enterica* serovar Typhimurium (*22*) or nigericin (*23*) to activate the NLRC4 or NLRP3 inflammasomes, respectively. *Salmonella* and nigericin induced rapid caspase-1-dependent pyroptosis of macrophages, which indeed requires GSDMD (**Fig. S1**), as previously reported (*1, 2*). In neutrophils, *Salmonella* and nigericin induced hallmarks of caspase-1 activation, such as caspase-1 self-processing to generate the inactive p20 fragment (**Fig. 1A-B**)(*24*) and IL-1β release (**Fig. S2**). Both *Salmonella* and nigericin induced some neutrophil death, however, death in these settings was not pyroptotic, as it was not driven by caspase-1 (*15*) or GSDMD (**Fig. 1C-D**). Thus, while canonical inflammasomes signal in neutrophils to drive IL-1β production, these cells do not die by pyroptosis.

To examine whether the non-canonical inflammasome is able to induce neutrophil pyroptosis, we primed neutrophils with the TLR1/2 agonist, Pam3CSK4, for 4 h to suppress basal neutrophil apoptosis and induce the expression of caspase-11, NLRP3 and pro-IL-1β. We then transfected LPS into the cytosol to activate caspase-11. Surprisingly, cytosolic LPS induced a modest but significant increase in neutrophil lactate dehydrogenase (LDH) release, in a caspase-11- and GSDMD-dependent manner (**Fig. 1E-F**), similar to the macrophage response (**Fig. S3**) (*1, 2, 9*).

Cytosolic LPS also induced caspase-11-dependent cleavage of GSDMD in neutrophils (**Fig. 1G**). In macrophages, caspase-11-dependent GSDMD signaling triggers a loss of cytosolic K^+, which in turn activates the NLRP3 inflammasome, leading to caspase-1-dependent IL-1β maturation and secretion, while cell death proceeds independently of NLRP3 (*9, 25*). Similar to macrophages, NLRP3 was dispensable for LPS-induced death of neutrophils (**Fig. 1H**), but was required for caspase-11/GSDMD-dependent IL-1β release (**Fig. 1I-K**). Culturing neutrophils in high extracellular potassium to prevent potassium efflux during caspase-11-driven neutrophil death suppressed NLRP3-dependent IL-1β cleavage and release (**Fig. 1L, Fig. S4).** These data indicate that the caspase-11-GSDMD-NLRP3 signaling axis is broadly conserved between neutrophils and macrophages, and neutrophils are susceptible to caspase-11-driven death.

Caspase-11, but not caspase-1, efficiently cleaves GSDMD

The observation that neutrophils are capable of dying via caspase-11 and GSDMD raises the question of how these cells resist caspase-1-dependent pyroptosis during canonical inflammasome signaling. To investigate the responsible mechanisms, we first examined LPS- and Pam3CSK4-primed macrophages and neutrophils for expression of key components of the pyroptosis pathway. Neutrophils expressed GSDMD at equivalent levels to macrophages, but expressed substantially less caspase-1 and caspase-11 (**Fig. 2A**). We next compared the ability of caspase-1 versus caspase-11 to cleave GSDMD to generate the p30 fragment that executes pyroptosis. GSDMD was effectively cleaved by recombinant caspase-11, but GSDMD cleavage by recombinant caspase-1 was markedly less efficient (**Fig. 2B**). Caspase-1 but not caspase-11 cleaved pro-IL-1β (**Fig. 2B**). To determine whether these differences in the capacity of caspase-1 versus caspase-11 to cleave GSDMD were also reflected in inflammasome-signaling neutrophils, we transfected neutrophils with flagellin or LPS, to activate the canonical or non-canonical inflammasomes, respectively. While both stimuli induced IL-1β secretion (**Fig. 1I-L, S5A**), LPS but not flagellin triggered strong GSDMD cleavage (**Fig. 2C**), and flagellin did not induce GSDMD-dependent cell death (**Fig. S5B**). We propose that the extent of GSDMD cleavage dictates the number of GSDMD-p30 pores that form in the membrane, and the latter must reach a certain threshold in order to overwhelm the neutrophil's natural membrane repair mechanisms, and induce cell death. Given that neutrophils express substantially less caspase-1 than

macrophages, and GSDMD is most efficiently cleaved by caspase-11, our data suggest that the abundance of these caspases and their relative efficiency for GSDMD cleavage dictates whether or not a cell dies by pyroptosis downstream of canonical and non-canonical inflammasomes. It remains possible that other mechanisms also contribute to the specific suppression of caspase-1-mediated GSDMD cleavage and pyroptotic cell death in neutrophils.

Neutrophil pyroptosis evokes the extrusion of neutrophil extracellular traps

With the hypothesis that pyroptosis and NETosis may be mechanistically linked, we examined LPS-transfected neutrophils for characteristics of NETosis. Cytosolic LPS triggered substantial NETosis in WT but not *Casp11*- or *Gsdmd*-deficient neutrophils, as observed by nuclear delobulation, DNA extrusion, DNA-MPO colocalization, and histone H3 citrullination (**Fig. 3A-B, S5C**). By contrast, Pam3CSK4-primed and mock-transfected neutrophils were generally negative for citrullinated histone, exhibited MPO staining in cytosolic granules, and the lobular nuclear structure characteristic of healthy neutrophils (**Fig. 3A, S5C-D**). Blinded image quantification scored cells as healthy or undergoing NETosis (which was defined as neutrophils with delobulated nuclei, or diffuse or extruded DNA), and objective image quantification in ImageJ also scored the extent of histone H3 citrullination. Cytosolic LPS induced NETosis in ~90% of WT neutrophils (**Fig. 3C**), and elicited caspase-11- and GSDMD-dependent histone H3 citrullination (H3Cit; **Fig. 3D**). In line with earlier observations that active caspase-1 does not trigger neutrophil pyroptosis or strong GSDMD cleavage (**Fig. 1A-D, 2C**) (*15*), transfection of the NLRC4 inflammasome agonist, flagellin, did not induce LDH release, NETosis or histone H3 citrullination (**Fig. 3C-D**; **Fig. S5**). In monitoring the kinetics of early versus late NETosis and histone citrullination in neutrophils stimulated with cytosolic LPS, we noted that histone citrullination occurs concurrently with early NETosis, as early as 2 h and peaking at 4 h, while DNA extrusion continues to rise throughout the 8 h time course (**Fig. S6**). *Casp11* and *Gsdmd*-deficient neutrophils failed to citrullinate histones or induce NETosis, even at late time points (e.g. 8 h) of cytosolic LPS exposure (**Fig. S6**). Thus, active caspase-11, but not active caspase-1, triggers neutrophil death and NET extrusion. Pyroptosis is defined as gasdermin-dependent cell death (*2*), but is morphologically distinct from NETosis, as the nuclear membrane remains intact in pyroptosis, but becomes compromised during NETosis. NETosis induced by classical

stimulants proceeds independently of caspases (*26*), but shares the morphological features of NETosis induced by caspase-11/GSDMD signaling. We thus termed this GSDMD-induced mode of neutrophil death, caspase-11-driven NETosis.

Caspase-11-induced NETosis proceeds independently of myeloperoxidase, neutrophil elastase, and protein arginine deiminase-4

While the signaling pathways driving and executing NETosis are not fully elucidated and may not be universally deployed by all NET-inducing stimuli (*27*), functions for NE (*18*), MPO (*18*), and PAD4 (*19, 20, 28*) are implicated in histone inactivation and resultant chromatin relaxation during the early stage of NETosis induced by specific classical stimuli. We took a genetic approach to examine the signaling requirements for caspase-11-induced NETosis. *Casp11* and *Gsdmd* deficiency blocked LPS-induced granule rupture and the resultant redistribution of MPO (**Fig. 3B**), suggesting that GSDMD pores may directly target and lyse granule membranes, which may provide a mechanism for NE and MPO to be liberated from granules to mediate histone degradation and chromatin decondensation. However, NE or MPO deficiency did not significantly affect caspase-11-driven NETosis, histone citrullination or GSDMD cleavage (**Fig. S7A-C**). Chromatin decondensation can also be mediated by PAD4, which is activated by a spike in cytosolic cytosolic calcium (*28*). PAD4 deficiency abrogated LPS-induced histone citrullination, but did not affect caspase-11-induced NETosis (**Fig. S7A-C**). The calcium chelator, EGTA, also blocked LPS-induced histone citrullination (**Fig. S7D**). As GSDMD pores enable calcium influx (*29*), this suggests that GSDMD pores facilitate calcium-dependent PAD4 activation and resultant histone citrullination; this accompanies, but is not absolutely required, for caspase-11-induced NETosis. As PAD4, NE and MPO were not required for LPS-induced NET extrusion, we thus sought to establish alternative mechanisms that may underlie the cellular changes required for caspase-11-driven NETosis.

Caspase-11 and GSDMD function coordinately to drive NETosis

Caspase-11 triggers macrophage pyroptosis by cleaving GSDMD to induce GSDMD-p30 pores in the plasma membrane. However, GSDMD-p30 is also inserted into internal cell membranes

(e.g. endosome, lysosome, Golgi) (*5*), with unknown functions. NETosis is associated with the sequential breakdown of multiple cell membranes; firstly, the neutrophil granule and nuclear membranes dissolve, allowing granular proteins and DNA to mix within the intact cell (early NETosis), and finally, the plasma membrane ruptures to allow DNA extrusion (late NETosis). To determine which of these stages may be directed by GSDMD pores, we quantified the proportion of neutrophils in early versus late NETosis from immunofluorescence images. Caspase-11 and GSDMD were required not only for DNA extrusion through the plasma membrane during late NETosis, but also for early stage NETosis (**Fig. 4A**). Of note, the number of WT neutrophils in late stage NETosis 4 h after LPS transfection (~14% with ruptured plasma membranes and extruded NETs; **Fig. 4A**) agreed well with LDH release at the same time point (**Fig. 1E,F**), consistent with a requirement for plasma membrane rupture for LDH release during neutrophil caspase-11-driven NETosis, as is the case during macrophage pyroptosis (*30*). As *Casp11*- and *Gsdmd*-deficient neutrophils showed a profound loss of both early and late NETosis (**Fig. 4A**), and their granules remained intact (**Fig. 3B**), this suggests that GSDMD-p30 pores may target the nuclear, granule and plasma membranes.

To determine whether GSDMD may exert functions in the nuclear membrane, we stimulated neutrophils with cytosolic LPS and prepared nuclear extracts. Immunoblot analysis confirmed that GSDMD-p30 was indeed recruited to the nucleus in a caspase-11-dependent manner (**Fig. 4B**). We hypothesized that GSDMD and caspase-11 may function in concert to promote nuclear delobulation and DNA expansion. For example, GSDMD-p30 pores may permeabilize the nuclear membrane, allowing caspase-11 to access the nuclear contents to perform an analogous function to NE, in which caspase-11 cleaves and inactivates histones to relax chromatin. Indeed, when recombinant caspase-11 was added to GSDMD to generate GSDMD-p30, and this mix was added to purified neutrophil nuclei, it permeabilized the nuclear membrane leading to uptake of the DNA dye SYTOX (**Fig. 4C**) and caused nuclear delobulation and DNA expansion (**Fig. 4D**), features of early NETosis. Full length GSDMD (i.e. not co-administered to nuclei with caspase-11) did not induce such features in neutrophil nuclei. Furthermore, when neutrophil nuclear extracts were exposed to recombinant caspase-11, caspase-11 specifically degraded histone H3 (**Fig. 4E**). These results suggest that caspase-11 and GSDMD together co-ordinate early and late NETosis. We propose that GSDMD-p30 pores dissolve the nuclear membrane, and in so doing

facilitate caspase-11-mediated nuclear changes, such as histone H3 degradation, leading to DNA expansion. GSDMD-p30 pores may then eventually trigger plasma membrane rupture as they do in macrophages, leading to the extrusion of the neutrophil's decondensed DNA.

A cytosolic Gram-negative bacterium induces NETosis of human neutrophils

We considered that LPS recognition by caspase-11 and resultant NETosis may be a mechanism for neutrophils to defend themselves against cytosolic invasion by Gram-negative bacteria. To test this, and provide proof-of-principle that this pathway operates in humans, we challenged primary blood neutrophils with *Citrobacter rodentium* that is well established to escape the phagosome and activate caspase-11 (*9*), which we employed here to activate the caspase-11 human ortholog, caspase-4. Similar to the well established NETosis activator, phorbol myristate acetate (PMA, **Fig. S8**), *Citrobacter rodentium* indeed triggered NETosis of human neutrophils, as detected by SYTOX uptake and chromatin externalization, and this was blocked by cell exposure to the caspase-1/4 inhibitor, VX765 (**Fig. 5**). Thus, human neutrophils launch an inflammasome-driven NETosis pathway in response to cytosolic invasion by Gram-negative bacteria.

Caspase-11-driven NETosis protects neutrophils from cytosolic bacterial invasion

NETs are well characterized to entrap and neutralize extracellular pathogens. We hypothesized that caspase-11-induced NETosis may be a defense pathway to restrict neutrophil cytosolic infection. To test this, we infected murine neutrophils with the *Salmonella* Typhimurium mutant, *ΔsifA,* which is well characterized to localize to the cytosol of infected macrophages, where it activates macrophage caspase-11 (*14*). As anticipated, neutrophil infection with *ΔsifA Salmonella* triggered NETosis and histone citrullination via caspase-11 and GSDMD (**Fig. 6A-C**). Image quantification of plasma membrane-labelled neutrophils revealed that GSDMD protected neutrophils from cytosolic infection, as *Gsdmd*$^{-/-}$ neutrophils were more frequently infected with bacteria and exhibited strikingly higher numbers of bacteria per infected cell, compared to WT neutrophils (**Fig. 6D**). Caspase-11-driven NETosis is thus a host defense

mechanism, which prevents bacteria from surviving, and potentially replicating, in the neutrophil cytosol.

Caspase-11/GSDMD-induced NETs mediates in vivo host defense

To determine whether caspase-11-induced NETosis provides host defense *in vivo*, we challenged mice with *Salmonella ΔsifA* via intraperitoneal injection. To test whether NETs kill bacteria and/or prevent bacterial dissemination to a secondary infection site in this context, we used established methods (*31*) to degrade extracellular DNA as NETs are extruded *in vivo*, by injecting mice with recombinant DNase I at 4 h post-infection. Bacterial dissemination to the spleen was assessed 24 h after infection. *Casp11* or *Gsdmd* deficiency resulted in increased splenic bacterial burden (**Fig. 6E**), confirming that non-canonical inflammasome signaling provides host defense against *Salmonella ΔsifA*, as was previously indicated by *ΔsifA* challenge in *Casp11*$^{-/-}$ mice (*14*). Consistent with an essential role for caspase-11-driven NETosis in host defense, DNase I application to dismantle NETs *in vivo* increased splenic bacterial burden in WT but not *Casp11*$^{-/-}$ or *Gsdmd*$^{-/-}$ mice (**Fig. 6E**). NETosis was also evident in the spleens of infected WT but not *Casp11*$^{-/-}$ mice at 48 h post-infection (**Fig. S9**). In all, these data demonstrate that a major *in vivo* function of caspase-11 and GSDMD is to prevent bacterial dissemination by driving NETosis and NET-dependent bacterial killing.

Discussion

NETosis is well appreciated to provide host defense against extracellular pathogens that cannot be efficiently phagocytosed (*32*). Until now, mechanisms protecting neutrophils from cytosolic invasion by pathogens were unclear. Here we demonstrate the surprising finding that cytosolic LPS and cytosolic Gram-negative bacteria trigger neutrophil caspase-11/GSDMD-dependent NET extrusion, and this protects neutrophils from cytosolic infection *in vitro*. Furthermore, caspase-11 provides *in vivo* host defense against cytosolic bacteria via the extrusion of GSDMD-dependent NETs. We thus reveal that caspase-11-driven NETosis is an antimicrobial pathway deployed against cytosolic Gram-negative pathogens that have evaded classical neutrophil defense mechanisms. Host defense by caspase-11-induced NETosis is likely mediated by

multiple coordinated antimicrobial programs (**Fig. S10**). Firstly, like pyroptosis, caspase-11-driven NETosis allows an infected cell to produce IL-1β and undergo cell lysis, leading to bacterial release. This will prevent bacterial survival and replication in the cytosol, and render bacteria susceptible to extracellular defense mechanisms, such as killing by IL-1β-recruited and activated neutrophils (*33*). Secondly, extruded NETs entrap bacteria to prevent their dissemination, and can be directly anti-bacterial (*3*). Caspase-11-induced NETosis thereby allows cytosolic bacteria to be neutralized upon the NET as they are released from their host neutrophil. Finally, GSDMD pores may directly target the bacterial cell wall to mediate bacteriolysis (*6*). Caspase-11-driven NETosis thus offers a multilayered defense strategy against bacteria that have invaded the neutrophil cytosol.

We, and others, previously reported that neutrophils are resistant to caspase-1-dependent pyroptosis (*15-17*), unlike macrophages, which readily die by caspase-1-driven pyroptosis. We show here that neutrophils are not intrinsically resistant to inflammasome-mediated lysis, as caspase-11 triggers robust GSDMD cleavage and neutrophil NETosis. Functions for GSDMD in mediating neutrophil lysis are also supported by a recent study, in which *in vitro* neutrophil ageing for 24 h triggered NE-dependent GSDMD cleavage and resultant neutrophil death (*34*). While it is possible that caspase-1 triggers a pyroptosis protection program in neutrophils (e.g. membrane repair mechanisms), our data suggest that the block in caspase-1-driven pyroptosis primarily occurs upstream of GSDMD pores, as caspase-1 appears unable to efficiently cleave GSDMD into the pore-forming p30 fragment in neutrophils. This is likely to be a consequence of relatively low caspase-1 expression in neutrophils, and the relatively poor efficiency of caspase-1 in cleaving GSDMD. In addition, the canonical inflammasome signaling adaptor, ASC, is expressed at much lower levels in neutrophils compared to macrophages, so inflammasome-activated neutrophils assemble a smaller inflammasome complex with reduced caspase-1 activity (*24*). In all, this suggests that caspase-1 activity in neutrophils is fine-tuned to enable sub-lytic GSDMD cleavage, presumably to facilitate IL-1β release (*35*), while resisting pyroptosis. This suggests that neutrophil viability during canonical inflammasome signaling is critical for host defense. This makes intuitive sense because infections that trigger canonical inflammasome activation are generally effectively cleared by the classical defense mechanisms of IL-1β-

recruited neutrophils (e.g. degranulation, phagocytosis, reactive oxygen species); such host-protective functions of neutrophils would be lost if neutrophils died by caspase-1-dependent pyroptosis. If under specific circumstances neutrophil caspase-1 can induce sufficient GSDMD cleavage for cell death induction, it remains an interesting question as to whether the cell would die by pyroptosis or NETosis. As caspase-1 only remains active when it is bound to the inflammasome (*24*), it is unlikely to be able to enter the nucleus to drive the nuclear changes required for NETosis, such as histone inactivation and DNA decondensation. Thus, we speculate that NETosis may be a cell death mode specific to neutrophils signaling via the non-canonical inflammasome.

NETosis is a multi-stage process involving nuclear and granule membrane breakdown, chromatin relaxation and mixing with granule proteins, and finally, the expulsion of decondensed chromatin from the cell. NETosis induced by classic stimuli (e.g. extracellular pathogens, PMA, ionomycin) proceeds independently of caspase activity and thus caspase-11 (*26*), and can be induced by at least two pathways that await full characterization. One pathway involves the ROS-dependent translocation of NE from granules into the nucleus, where NE induces histone degradation and chromatin decondensation (*18*). This pathway is elicited by mitogens (e.g. PMA), cholesterol crystals and extracellular pathogens (e.g. *C. albicans*, group B *Streptococci*) (*18*), and the accompanying report shows that this pathway triggers NE-dependent GSDMD cleavage, and requires GSDMD-p30 pores for rupture of the granule and plasma membranes, and subsequent NET extrusion (*36*). In an alternative pathway, the enzyme PAD4 is activated by a spike in cytosolic calcium, and triggers histone citrullination to promote chromatin decondensation (*19*). Here, we describe a surprising signaling pathway leading to NET extrusion (**Fig. S10**). In contrast to NETosis induced by classic stimulants such as extracellular pathogens, caspase-11-driven NETosis is elicited by the LPS of cytosolic Gram-negative bacteria, and proceeds independently of NE, MPO and PAD4. Caspase-11-driven NETosis, does however, converge with the NE-driven NETosis signaling pathway as both lead to the cleavage and activation of the NETosis executioner protein, GSDMD. LPS binds to, and activates, caspase-4/11 within the non-canonical inflammasome complex, leading to GSDMD cleavage, pore formation and membrane perforation. Previous studies have characterized GSDMD pores in the macrophage plasma membrane, where they interact with the phosphoinositide, PI(4,5)P2, in the

inner leaflet (*5, 6*), and mediate cell rupture (*1, 2, 4-8, 29*). Here we show in neutrophils previously uncharacterized functions for GSDMD in targeting the nuclear envelope. The phospholipid content of the nuclear membrane is surprisingly ill-defined, but several reports suggest it contains PI(4,5)P2, including in neutrophils (*37, 38*), suggesting a potential mechanism for GSDMD-p30 nuclear membrane recruitment in neutrophils. Our data indicate that the combined actions of GSDMD and caspase-11 drive nuclear permeabilization, chromatin relaxation and plasma membrane rupture during LPS-induced NETosis. Mechanistically, our data suggest that GSDMD pores in the nuclear membrane allow nuclear membrane breakdown and caspase-11 access to chromatin, wherein caspase-11 performs an analogous function to NE, mediating histone clipping and inactivation to enable DNA expansion. During caspase-11-driven NETosis, PAD4 becomes activated, likely via calcium influx through GSDMD pores, and PAD4 citrullinates histone H3; this accompanies but is not required for NETosis. Thus while caspase-11-induced NETosis and classical NE-driven NETosis are morphologically similar, they occur in response to distinct challenges via different signaling mechanisms that converge on a common executioner protein, GSDMD.

In addition to their host-protective functions, NETs can drive pathology in a multitude of inflammatory, autoimmune and other diseases, such as sepsis, lupus, rheumatoid arthritis, vasculitis, type 1 diabetes, gout, preeclampsia, periodontitis, and cancer (*21, 39*). A gasdermin family member closely related to GSDMD, GSDME, was recently shown to execute pyroptosis during chemotherapy (*40*) and uncontrolled apoptosis (*41*). NETs can promote cancer progression (*39*), and lupus patients show defects in apoptotic cell clearance (*42*). Characterizing functions for GSDMD and GSDME in driving NETosis during autoimmune and other inflammation-linked diseases could thus reveal these molecules as new therapeutic targets for such conditions.

Materials and Methods

Study design

This study aimed to define inflammasome signaling pathways leading to GSDMD-dependent neutrophil death by NETosis and anti-bacterial host defense. To do this, we challenged murine and human neutrophils with inflammasome agonists and bacteria *in vitro*, and monitored inflammasome signaling outputs (cleavage and/or release of caspase-1, GSDMD, IL-1β), cell lysis (LDH release) and NETosis (microscopy, SYTOX uptake). The contribution of caspase-11-dependent NETs to host defense was assessed by murine *in vivo* challenge with Δ*sifA Salmonella*. Signaling pathways were mapped through the use of gene-deficient mice, or the application of specific inhibitors. Where image quantification required manual image scoring, images were blinded and randomized prior to their analysis by a researcher not involved in image acquisition. No other formal randomization or blinding method was used elsewhere in the study. The number of independent replicates for each experiment is outlined in the figure captions.

Bacterial strains

Salmonella enterica serovar Typhimurium SL1344 strains and *Citrobacter rodentium* were grown overnight at 37^{o}C in Luria-Bertani broth at 200 rpm (stationary phase). To induce *Salmonella* SPI1-T3SS expression, overnight bacteria were diluted 1:40 and grown for 3 h (log phase). The SL1344 *ΔsifA* mutant was generated using the λ Red-mediated homologous recombination system (*43*). mCherry-expressing SL1344 *ΔsifA* was generated by electroporation of the low copy plasmid pFPV-mCherry (Addgene), and used for some imaging experiments.

Mice

All experiments were performed with age- and sex-matched mouse cohorts. C57BL/6, *Casp11*$^{-/-}$ *(9, 44), Gsdmd*$^{-/-}$ *(1, 45)*, *Ne*$^{-/-}$ *(46)*, *Mpo*$^{-/-}$*(47)*, *Pad4*$^{-/-}$ (*48*) mice were housed in specific pathogen-free facilities at the University of Queensland or the University of Lausanne. All animal experiments were performed with approval from The University of Queensland's animal

ethics committee or the veterinary office of the Canton de Vaud and Swiss animal protection law (license VD3257).

Murine primary macrophage and neutrophil preparation and stimulation

Mature neutrophils were purified from murine bone marrow using magnetic-assisted cell sorting (MACS) and used for experiments immediately after purification, while bone marrow progenitors were differentiated with recombinant human colony-stimulating factor-1 (CSF-1) over 7 days to generate macrophages, as previously described (*15*).

Inflammasome assays

Neutrophils were seeded at a density of 1 x 10^7 cells/ml in Opti-MEM (Life Technologies) supplemented with 4 μg/ml aprotinin (Sigma). Differentiated macrophages were seeded at a density of 1 x 10^6 cells/ml in RPMI-1640 supplemented with 10% heat-inactivated FCS, Glutamax (Life Technologies), and 150 ng/ml recombinant human CSF-1 (endotoxin-free, produced in insect cells by the UQ Protein Expression Facility) on day 6, and cell culture media was replaced for CSF-1-supplemented Opti-MEM on day 7 of differentiation. Cells were primed with 100 ng/ml ultrapure LPS or 1 μg/ml Pam3CSK4 (Invivogen) for 4 h. Cells were then transfected with 2-10 μg/ml ultrapure *E. coli* K12 LPS (Invivogen) or 1 μg/ml ultrapure flagellin (Invivogen) using 0.25% FuGene HD (Promega) and centrifuged at 700 *g* for 10 min at room temperature, or stimulated with 5 μM nigericin. IL-1β in cell-free supernatants was quantified by ELISA (eBioscience). Cell extracts and methanol/chloroform-precipitated cell-free supernatants were analyzed by immunoblot as previously described (*15*), using antibodies against caspase-1 (Casper-1, Adipogen), caspase-11 (EPR18628, Abcam), IL-1β (AF-401-NA, R&D systems), GSDMD (EPR19828; Abcam), Histone H3 (96C10, Cell Signaling Technology) and GADPH (polyclonal rabbit, BioScientific). LDH release into the cell culture supernatant was quantified using CytoTox 96® non-radioactive cytotoxicity assay (Promega).

Murine neutrophil and macrophage in vitro infection assays

Cells were primed with 100 ng/ml ultrapure *E. coli* K12 LPS (Invivogen) or 1 μg/ml Pam3CSK4 (Invivogen) for 4 h. Cells were then infected with wild-type *Salmonella* SL1344 or isogenic Δ*sifA* at an MOI of 25 (neutrophils) or 10 (macrophages), and centrifuged immediately at 700 *g* for 10 min at room temperature. Cells were then incubated at 37°C for 25 min to allow bacterial uptake, before adding 100 μg/ml gentamicin (Life Technologies) to the culture media for the remainder of the assay to kill extracellular bacteria. For microscopy, stationary-phase grown bacteria were opsonized for 15 minutes at 37°C with 10% rat serum, and added to neutrophils at an MOI of 50. Infection was allowed to proceed for 40 minutes, then cells were washed twice with Opti-MEM and cell culture medium was replaced with medium containing 20 μg/ml gentamicin for the remainder of the assay. Cells were then further incubated for the indicated times before harvesting cell-free supernatants and cell lysates for cytokine and LDH release assays, or fixed in paraformaldehyde (PFA) for imaging.

Deconvolution immunofluorescence microscopy

Neutrophils were plated on 0.0001% poly-L-Lysine coated glass coverslips at 1 x 10^6 cell/ml, and fixed in 2% PFA for 15 min at 37°C. Cells were permeabilized in 0.1% Triton X-100 for 10 min, blocked in 0.5% BSA for 30 min and incubated with primary and respective secondary antibodies for 1 h. Primary antibodies used were H3Cit (ab5103; Abcam) and MPO (goat polyclonal; R&D systems). Alexa Fluor -488, -594 and 647 were purchased from Molecular Probes. Coverslips were mounted with ProLong Gold Reagent (Life Technologies). Z-stacks were imaged using a DeltaVision Olympus IX80 inverted wide-field deconvolution microscope equipped with Olympus U-Apochromat x40/1.35, Plan-Apochromat x60/1.35 or UPLS-Apochromat x100/1.4 oil lenses and a Lumencor 7 line LED lamp. Images were captured using a Photometrics Coolsnap HQ2 camera. Images were deconvolved using 10 cycles of conservative iterative deconvolution using SofWorx. Image analysis was performed using ImageJ software. The percentage of neutrophils with citrullinated histone H3 and undergoing NETosis was quantified via image analysis of five to seven non-overlapping fields of view (60x; in which each field of view contained approximately 20-25 cells) for each treatment and genotype for each of three biological replicates (>300 cells total for each condition) unless otherwise indicated. To

quantify histone H3 citrullination, deconvolved images were subjected to quantitative analysis with a custom ImageJ macro script. Images were maximum intensity projected, split into individual channels and subject to 100 pixel rolling ball background subtraction. Total cell number in each field of view was determined by counting intensity thresholded (250-65535) DAPI (nuclear) labeling and using size exclusion to eliminate noise, while H3 positive cells were subjected to 100 pixel rolling ball background subtraction and median filtering (radius =2 pixels). High intensity labeled cells were selected as positive via thresholding (750:65535). The percentage of cells undergoing NETosis was determined by blinded manual counting, in which those cells with delobulated nuclei or diffuse DNA (early NETosis) or spread extracellular DNA (late NETosis) were identified from DAPI-stained blinded images. For analysis of intracellular bacteria, deconvolved images of WGA-680/DAPI-stained, infected neutrophils were split into individual channels. Total number of cells per field of view was determined in ImageJ using DAPI as above, and infected cells and numbers of bacteria per cell were enumerated by analysis of mCherry-positive bacteria that were clearly confined within WGA-stained cells.

Isolation and NETosis of human primary neutrophils

Blood was taken from healthy human volunteers with written informed consent, with the approval of the Charité-Universitätsmedizin Berlin Ethics Committee and in accordance with the Declaration of Helsinki. Neutrophils were isolated as previously described (*26*), and seeded at 10^6/ml in RPMI (without phenol red) supplemented with 10 mM HEPES and 0.02% human serum albumin in a 96-well plate. Neutrophils were primed for 2 h with 1 μg/ml Pam3CSK4. Where indicated, 50 μM VX765 (Invivogen) was added to cells during the final 30 min of priming. Neutrophils were challenged with stationary phase *Citrobacter rodentium* at the indicated MOI and centrifuged immediately for 10 min at 300 *g* and incubated 37°C for a further 30 min to allow phagocytosis. 100 μg/ml gentamicin was then added to the culture medium to kill extracellular bacteria. After 30 min, the culture medium was replaced with fresh media containing 50 nM SYTOX Green (Invitrogen). Neutrophils were also stimulated with 100 nM PMA as a positive control for NETosis, and analyzed as above. Cell death was quantified over time by measuring fluorescence intensity using a fluoroscan plate reader (excitation/emission 485/518) and acquiring pictures at an EVOS microscope. Pam3CSK4-primed neutrophils

infected at MOI 10 for 2.5 h were also assessed for NETosis by confocal microscopy. Cells were fixed by pH shift fixation (3% PFA k-PIPES 80 mM pH 6.8, for 5 mins followed by 3% PFA Borax 100 mM for 10 mins). After washing with PBS, cells were permeabilized with 0.1 % Triton-X100 for 5 min at 4 °C, and blocked with 3% BSA for 1 h. Cells were then incubated overnight at 4 °C with primary antibodies (anti-MPO, Dako, A0398; anti-chromatin PL2.3 (*49*)). After 3 washes with PBS, secondary antibodies were added for 30 mins in 3% BSA, and DNA was counterstained with 1 μg/ ml DAPI. After 3 further PBS washes, images were acquired using a Leica SP8 confocal microscope.

In vivo infection

Mice were challenged i.p. with 1 x 10^5 CFU of the *Salmonella* Typhimurium *ΔsifA* mutant grown to stationary phase. At 4 h post-infection, mice were administered 150 U cell culture-grade DNase I (Roche) i.p., to degrade NETs. Mice were sacrificed at 24 h post infection for determination of splenic bacterial burden by serial dilution, or at 48 h post infection for spleen fixation in 4% PFA for 24 h at 4^{o}C, followed by paraffin embedding.

Immunofluorescence staining of fixed tissue

Immunofluorescence was performed on 7 μm spleen sections. Sections were de-waxed using xylene and rehydrated in a gradient of ethanol (100, 95, 80 and 70%). Antigen unmasking was performed by boiling the slides in sodium citrate buffer (10 mM Tri-sodium citrate, 0.05% Tween, pH 6.0) for 10 mins. Slides were then blocked (5% FCS, 0.3% Triton X-100 in PBS). Slides were incubated in primary antibodies overnight (rabbit anti-H3Cit, goat anti-MPO) in blocking buffer, and then incubated for 1 h with secondary antibodies (anti-rabbit Alexa -594 and anti-goat Alexa -488). Slides were then stained with DAPI for 10 min, mounted using Dako mounting media (Dako), and sealed. Images were captured at 63X using oil immersion with Carl Zeiss Meta Inverted LSM 510 microscope (Carl Ziess) and processed using ImageJ.

Recombinant protein expression

Murine caspases were expressed with C-terminal His_8 tags in *E. coli* BL21 Gold. ΔCARD_caspase-1 was expressed as a GST-DmrB fusion protein, and expression was induced with 200 μM IPTG for 8h at 18°C. Caspase-11 expression was induced with 200 μM IPTG for 6 h at 30°C. ΔCARD_caspase-1 and caspase-11 were purified using Ni Sepharose 6 Fast Flow resin as described (*50*). Active caspase concentration was quantified via active site titration using zVAD-fmk (*50*). Murine GSDMD was expressed as a GST fusion protein in *E.coli* BL21, and expression was induced with 200 μM IPTG for 12 h. GST-GSDMD was purified using MagneGST gluthatione beads (Promega), where GSDMD was cleaved from GST using 3C protease (expressed in house) and eluted in PBS. GSDMD concentration was determined using the Beer-Lambert law.

Neutrophil fractionation

Neutrophils were fractionated into cytosolic versus nuclear extracts using standard techniques. Briefly, 4 million neutrophils were incubated with 150 μL hypotonic buffer (10 mM HEPES pH 8.0, 10 mM KCl, 3 mM NaCl, 3 mM $MgCl_2$, 1 mM EDTA, 1 mM EGTA, 2 mM DTT, 2 mM PMSF, cOmplete mini protease inhibitor cocktail, Roche) and incubated on ice for 15 mins. IGEPAL was then added to a final concentration of 0.5%, and the cells were gently vortexted and then centrifuged at 500 *g* for 10 mins at 4 °C. The cytoplasmic (soluble) fraction was removed, and the pellet (nuclear fraction) was washed once more with hypotonic buffer before resuspension in western loading dye.

Assays with neutrophil nuclei

Nuclei were prepared from murine neutrophils primed for 4 h with 1 μg/mL Pam3CSK4. Cells were centrifuged at 400 *g* for 5 mins, resuspended in lysis buffer (100 mM KCl, 1 mM NaCl, 1 mM $ATP.Na_2$, 3.5 mM $MgCl_2$, 10 mM PIPES, 0.5 mM PMSF, cOmplete mini protease inhibitor cocktail, Roche) at 5 x 10^7 cells/mL and disrupted by nitrogen cavitation at 380 p.s.i. for 5 mins at 4 °C before centrifugation at 500 *g* for 5 mins at 4 °C. The pellet was washed with lysis buffer and again centrifuged. Nuclei were gently resuspended at 1 x 10^6 cells/mL in assay buffer (200

mM NaCl, 50 mM KCl, 50 mM HEPES pH 8.0, 10 mM DTT) and plated in a 96 well plate. 100 nM SYTOX green nucleic acid stain (ThermoFisher Scientific) was added to each well 15 mins prior to imaging. Recombinant proteins (2 μM full length GSDMD and/or 100nM caspase-11) were added to wells immediately prior to live cell imaging using a Nikon deconvolution microscope in a 37 °C chamber. Imaris (Bitplane) software quantified SYTOX volume and sum mean intensity of each cell.

Caspase cleavage assays

2 μM active site-titrated, recombinant caspase-1 and -11 were incubated in high salt buffer (50 mM HEPES pH 7.4, 50 mM NaCl, 1 M sodium citrate, 0.01% CHAPS, 10 mM DTT) for 30 mins to promote dimerization. Caspases were then serially diluted in caspase buffer (100 mM NaCl, 10 mM PIPES at pH 7.3, 10 % w/v sucrose, 0.1 % w/v CHAPS, 10 mM DTT) and incubated for 30 min at 37°C with cytosolic extracts from HEK293T cells overexpressing V5-tagged murine GSMDM or pro-IL-1β. Alternatively, caspase-11 was added to neutrophil nuclear extracts. For this, nuclei were isolated as above, and then incubated for 20 mins on ice in nuclear lysis buffer (20 mM HEPES pH 7.5, 25% glycerol, 0.8 M KCl, 1 mM $MgCl_2$, 1% IGEPAL CA-680, 0.5 mM EDTA, 2 mM DTT, 0.5 mM PMSF). The nuclear extract was cleared by centrifugation at 14 000 *g* for 15 mins at 4 °C, and then diluted in caspase buffer. SDS-PAGE loading dye was added to quench cleavage reactions, and samples boiled for 5 min before analysis by immunoblot.

Statistical analyses

Statistical analyses were performed using Prism GraphPad software. Data were analyzed for normality using the Shapiro-Wilk normality test. Statistical analyses on normally distributed data sets were performed using parametric t-tests (two-sided) while data sets with non-normal distributions were analyzed using nonparametric Mann-Whitney t-tests (two-sided). For repeated measures over time, 2-way ANOVA was performed. *In vivo* experiments were analyzed using the Mann-Whitney test. Data were considered significant when $p \leq 0.05$ (*), 0.01 (**), 0.001(***), or 0.0001(****).

Supplementary Materials

Fig. S1. GSDMD mediates rapid macrophage pyroptosis.

Fig. S2. *Salmonella* Typhimurium and nigericin induce IL-1β secretion from WT neutrophils.

Fig. S3. Cytosolic LPS triggers caspase-11-dependent cell death and IL-1β production from macrophages.

Fig. S4. Extracellular potassium blocks non-canonical NLRP3 activation and resultant release of mature IL-1β.

Fig. S5. Cytosolic LPS but not mock or flagellin transfection triggers GSDMD-dependent cell death.

Fig. S6. Time course analysis profiles the kinetics of caspase-11/GSDMD-induced NETosis.

Fig. S7. NE, MPO, and PAD4 are dispensable for GSDMD cleavage and caspase-11-driven NETosis.

Fig. S8. PMA induces NETosis of human neutrophils.

Fig. S9. Cytosolic bacteria triggers caspase-11-dependent NETs *in vivo*.

Fig. S10. Model for LPS-driven NETosis via GSDMD during cytosolic infection.

Table S1. Raw data file.

References and Notes

1. N. Kayagaki, I. B. Stowe, B. L. Lee, K. O'Rourke, K. Anderson, S. Warming, T. Cuellar, B. Haley, M. Roose-Girma, Q. T. Phung, P. S. Liu, J. R. Lill, H. Li, J. Wu, S. Kummerfeld, J. Zhang, W. P. Lee, S. J. Snipas, G. S. Salvesen, L. X. Morris, L. Fitzgerald, Y. Zhang, E. M. Bertram, C. C. Goodnow, V. M. Dixit, Caspase-11 cleaves gasdermin D for non-canonical inflammasome signalling. *Nature* **526**, 666-671 (2015).
2. J. Shi, Y. Zhao, K. Wang, X. Shi, Y. Wang, H. Huang, Y. Zhuang, T. Cai, F. Wang, F. Shao, Cleavage of GSDMD by inflammatory caspases determines pyroptotic cell death. *Nature* **526**, 660-665 (2015).
3. V. Brinkmann, U. Reichard, C. Goosmann, B. Fauler, Y. Uhlemann, D. S. Weiss, Y. Weinrauch, A. Zychlinsky, Neutrophil extracellular traps kill bacteria. *Science* **303**, 1532-1535 (2004).
4. R. A. Aglietti, A. Estevez, A. Gupta, M. G. Ramirez, P. S. Liu, N. Kayagaki, C. Ciferri, V. M. Dixit, E. C. Dueber, GsdmD p30 elicited by caspase-11 during pyroptosis forms pores in membranes. *Proc Natl Acad Sci U S A* **113**, 7858-7863 (2016).
5. J. Ding, K. Wang, W. Liu, Y. She, Q. Sun, J. Shi, H. Sun, D. C. Wang, F. Shao, Pore-forming activity and structural autoinhibition of the gasdermin family. *Nature* **535**, 111-116 (2016).
6. X. Liu, Z. Zhang, J. Ruan, Y. Pan, V. G. Magupalli, H. Wu, J. Lieberman, Inflammasome-activated gasdermin D causes pyroptosis by forming membrane pores. *Nature* **535**, 153-158 (2016).
7. L. Sborgi, S. Ruhl, E. Mulvihill, J. Pipercevic, R. Heilig, H. Stahlberg, C. J. Farady, D. J. Muller, P. Broz, S. Hiller, GSDMD membrane pore formation constitutes the mechanism of pyroptotic cell death. *EMBO J* **35**, 1766-1778 (2016).
8. W. T. He, H. Wan, L. Hu, P. Chen, X. Wang, Z. Huang, Z. H. Yang, C. Q. Zhong, J. Han, Gasdermin D is an executor of pyroptosis and required for interleukin-1beta secretion. *Cell Res* **25**, 1285-1298 (2015).
9. N. Kayagaki, S. Warming, M. Lamkanfi, L. Vande Walle, S. Louie, J. Dong, K. Newton, Y. Qu, J. Liu, S. Heldens, J. Zhang, W. P. Lee, M. Roose-Girma, V. M. Dixit, Non-canonical inflammasome activation targets caspase-11. *Nature* **479**, 117-121 (2011).

10. N. Kayagaki, M. T. Wong, I. B. Stowe, S. R. Ramani, L. C. Gonzalez, S. Akashi-Takamura, K. Miyake, J. Zhang, W. P. Lee, A. Muszynski, L. S. Forsberg, R. W. Carlson, V. M. Dixit, Noncanonical inflammasome activation by intracellular LPS independent of TLR4. *Science* **341**, 1246-1249 (2013).
11. J. Shi, Y. Zhao, Y. Wang, W. Gao, J. Ding, P. Li, L. Hu, F. Shao, Inflammatory caspases are innate immune receptors for intracellular LPS. *Nature* **514**, 187-192 (2014).
12. P. J. Baker, D. Boucher, D. Bierschenk, C. Tebartz, P. G. Whitney, D. B. D'Silva, M. C. Tanzer, M. Monteleone, A. A. Robertson, M. A. Cooper, S. Alvarez-Diaz, M. J. Herold, S. Bedoui, K. Schroder, S. L. Masters, NLRP3 inflammasome activation downstream of cytoplasmic LPS recognition by both caspase-4 and caspase-5. *Eur J Immunol* **45**, 2918-2926 (2015).
13. E. A. Miao, I. A. Leaf, P. M. Treuting, D. P. Mao, M. Dors, A. Sarkar, S. E. Warren, M. D. Wewers, A. Aderem, Caspase-1-induced pyroptosis is an innate immune effector mechanism against intracellular bacteria. *Nat Immunol* **11**, 1136-1142 (2010).
14. Y. Aachoui, I. A. Leaf, J. A. Hagar, M. F. Fontana, C. G. Campos, D. E. Zak, M. H. Tan, P. A. Cotter, R. E. Vance, A. Aderem, E. A. Miao, Caspase-11 protects against bacteria that escape the vacuole. *Science* **339**, 975-978 (2013).
15. K. W. Chen, C. J. Gross, F. V. Sotomayor, K. J. Stacey, J. Tschopp, M. J. Sweet, K. Schroder, The neutrophil NLRC4 inflammasome selectively promotes IL-1beta maturation without pyroptosis during acute Salmonella challenge. *Cell Rep* **8**, 570-582 (2014).
16. F. Martin-Sanchez, C. Diamond, M. Zeitler, A. I. Gomez, A. Baroja-Mazo, J. Bagnall, D. Spiller, M. White, M. J. Daniels, A. Mortellaro, M. Penalver, P. Paszek, J. P. Steringer, W. Nickel, D. Brough, P. Pelegrin, Inflammasome-dependent IL-1beta release depends upon membrane permeabilisation. *Cell Death Differ* **23**, 1219-1231 (2016).
17. M. Karmakar, M. Katsnelson, H. A. Malak, N. G. Greene, S. J. Howell, A. G. Hise, A. Camilli, A. Kadioglu, G. R. Dubyak, E. Pearlman, Neutrophil IL-1beta processing induced by pneumolysin is mediated by the NLRP3/ASC inflammasome and caspase-1 activation and is dependent on K+ efflux. *J Immunol* **194**, 1763-1775 (2015).

18. V. Papayannopoulos, K. D. Metzler, A. Hakkim, A. Zychlinsky, Neutrophil elastase and myeloperoxidase regulate the formation of neutrophil extracellular traps. *J Cell Biol* **191**, 677-691 (2010).
19. Y. Wang, M. Li, S. Stadler, S. Correll, P. Li, D. Wang, R. Hayama, L. Leonelli, H. Han, S. A. Grigoryev, C. D. Allis, S. A. Coonrod, Histone hypercitrullination mediates chromatin decondensation and neutrophil extracellular trap formation. *J Cell Biol* **184**, 205-213 (2009).
20. P. Li, M. Li, M. R. Lindberg, M. J. Kennett, N. Xiong, Y. Wang, PAD4 is essential for antibacterial innate immunity mediated by neutrophil extracellular traps. *J Exp Med* **207**, 1853-1862 (2010).
21. N. Branzk, V. Papayannopoulos, Molecular mechanisms regulating NETosis in infection and disease. *Semin Immunopathol* **35**, 513-530 (2013).
22. S. Mariathasan, K. Newton, D. M. Monack, D. Vucic, D. M. French, W. P. Lee, M. Roose-Girma, S. Erickson, V. M. Dixit, Differential activation of the inflammasome by caspase-1 adaptors ASC and Ipaf. *Nature* **430**, 213-218 (2004).
23. S. Mariathasan, D. S. Weiss, K. Newton, J. McBride, K. O'Rourke, M. Roose-Girma, W. P. Lee, Y. Weinrauch, D. M. Monack, V. M. Dixit, Cryopyrin activates the inflammasome in response to toxins and ATP. *Nature* **440**, 228-232 (2006).
24. D. Boucher, M. Monteleone, R. C. Coll, K. W. Chen, C. M. Ross, J. L. Teo, G. A. Gomez, C. L. Holley, D. Bierschenk, K. J. Stacey, A. S. Yap, J. S. Bezbradica, K. Schroder, Caspase-1 self-cleavage is an intrinsic mechanism to terminate inflammasome activity. *J Exp Med* **215**, 827-840 (2018).
25. S. Ruhl, P. Broz, Caspase-11 activates a canonical NLRP3 inflammasome by promoting K(+) efflux. *Eur J Immunol* **45**, 2927-2936 (2015).
26. T. A. Fuchs, U. Abed, C. Goosmann, R. Hurwitz, I. Schulze, V. Wahn, Y. Weinrauch, V. Brinkmann, A. Zychlinsky, Novel cell death program leads to neutrophil extracellular traps. *J Cell Biol* **176**, 231-241 (2007).
27. E. F. Kenny, A. Herzig, R. Kruger, A. Muth, S. Mondal, P. R. Thompson, V. Brinkmann, H. V. Bernuth, A. Zychlinsky, Diverse stimuli engage different neutrophil extracellular trap pathways. *Elife* **6**, (2017).

28. H. D. Lewis, J. Liddle, J. E. Coote, S. J. Atkinson, M. D. Barker, B. D. Bax, K. L. Bicker, R. P. Bingham, M. Campbell, Y. H. Chen, C. W. Chung, P. D. Craggs, R. P. Davis, D. Eberhard, G. Joberty, K. E. Lind, K. Locke, C. Maller, K. Martinod, C. Patten, O. Polyakova, C. E. Rise, M. Rudiger, R. J. Sheppard, D. J. Slade, P. Thomas, J. Thorpe, G. Yao, G. Drewes, D. D. Wagner, P. R. Thompson, R. K. Prinjha, D. M. Wilson, Inhibition of PAD4 activity is sufficient to disrupt mouse and human NET formation. *Nat Chem Biol* **11**, 189-191 (2015).

29. X. Chen, W. T. He, L. Hu, J. Li, Y. Fang, X. Wang, X. Xu, Z. Wang, K. Huang, J. Han, Pyroptosis is driven by non-selective gasdermin-D pore and its morphology is different from MLKL channel-mediated necroptosis. *Cell Res* **26**, 1007-1020 (2016).

30. L. DiPeso, D. X. Ji, R. E. Vance, J. V. Price, Cell death and cell lysis are separable events during pyroptosis. *Cell Death Discov* **3**, 17070 (2017).

31. A. Warnatsch, M. Ioannou, Q. Wang, V. Papayannopoulos, Inflammation. Neutrophil extracellular traps license macrophages for cytokine production in atherosclerosis. *Science* **349**, 316-320 (2015).

32. N. Branzk, A. Lubojemska, S. E. Hardison, Q. Wang, M. G. Gutierrez, G. D. Brown, V. Papayannopoulos, Neutrophils sense microbe size and selectively release neutrophil extracellular traps in response to large pathogens. *Nat Immunol* **15**, 1017-1025 (2014).

33. K. W. Chen, K. Schroder, Antimicrobial functions of inflammasomes. *Curr Opin Microbiol* **16**, 311-318 (2013).

34. H. Kambara, F. Liu, X. Zhang, P. Liu, B. Bajrami, Y. Teng, L. Zhao, S. Zhou, H. Yu, W. Zhou, L. E. Silberstein, T. Cheng, M. Han, Y. Xu, H. R. Luo, Gasdermin D Exerts Anti-inflammatory Effects by Promoting Neutrophil Death. *Cell Rep* **22**, 2924-2936 (2018).

35. R. Heilig, M. S. Dick, L. Sborgi, E. Meunier, S. Hiller, P. Broz, The Gasdermin-D pore acts as a conduit for IL-1beta secretion in mice. *Eur J Immunol*, (2017).

36. G. Sollberger, A. Choidas, G. L. Burn, P. Habenberger, R. D. Lucrezia, S. Kordes, S. Menninger, J. Eickhoff, P. Nussbaumer, B. Klebl, R. Krüger, A. Herzig, A. Zychlinsky, Gasdermin D is a key executioner in the formation of neutrophil extracellular traps. *Science Immunology*, in press (2018).

37. S. Choi, N. Thapa, X. Tan, A. C. Hedman, R. A. Anderson, PIP kinases define PI4,5P(2)signaling specificity by association with effectors. *Biochim Biophys Acta* **1851**, 711-723 (2015).
38. V. P. Sharma, V. DesMarais, C. Sumners, G. Shaw, A. Narang, Immunostaining evidence for PI(4,5)P2 localization at the leading edge of chemoattractant-stimulated HL-60 cells. *J Leukoc Biol* **84**, 440-447 (2008).
39. S. K. Jorch, P. Kubes, An emerging role for neutrophil extracellular traps in noninfectious disease. *Nat Med* **23**, 279-287 (2017).
40. Y. Wang, W. Gao, X. Shi, J. Ding, W. Liu, H. He, K. Wang, F. Shao, Chemotherapy drugs induce pyroptosis through caspase-3 cleavage of a gasdermin. *Nature* **547**, 99-103 (2017).
41. C. Rogers, T. Fernandes-Alnemri, L. Mayes, D. Alnemri, G. Cingolani, E. S. Alnemri, Cleavage of DFNA5 by caspase-3 during apoptosis mediates progression to secondary necrotic/pyroptotic cell death. *Nat Commun* **8**, 14128 (2017).
42. L. E. Munoz, C. van Bavel, S. Franz, J. Berden, M. Herrmann, J. van der Vlag, Apoptosis in the pathogenesis of systemic lupus erythematosus. *Lupus* **17**, 371-375 (2008).
43. K. A. Datsenko, B. L. Wanner, One-step inactivation of chromosomal genes in Escherichia coli K-12 using PCR products. *Proc Natl Acad Sci U S A* **97**, 6640-6645 (2000).
44. S. Wang, M. Miura, Y. K. Jung, H. Zhu, E. Li, J. Yuan, Murine caspase-11, an ICE-interacting protease, is essential for the activation of ICE. *Cell* **92**, 501-509 (1998).
45. J. C. Santos, M. S. Dick, B. Lagrange, D. Degrandi, K. Pfeffer, M. Yamamoto, E. Meunier, P. Pelczar, T. Henry, P. Broz, LPS targets host guanylate-binding proteins to the bacterial outer membrane for non-canonical inflammasome activation. *EMBO J* **37**, (2018).
46. A. Belaaouaj, R. McCarthy, M. Baumann, Z. Gao, T. J. Ley, S. N. Abraham, S. D. Shapiro, Mice lacking neutrophil elastase reveal impaired host defense against gram negative bacterial sepsis. *Nat Med* **4**, 615-618 (1998).
47. M. L. Brennan, M. M. Anderson, D. M. Shih, X. D. Qu, X. Wang, A. C. Mehta, L. L. Lim, W. Shi, S. L. Hazen, J. S. Jacob, J. R. Crowley, J. W. Heinecke, A. J. Lusis,

Increased atherosclerosis in myeloperoxidase-deficient mice. *J Clin Invest* **107**, 419-430 (2001).

48. S. Hemmers, J. R. Teijaro, S. Arandjelovic, K. A. Mowen, PAD4-mediated neutrophil extracellular trap formation is not required for immunity against influenza infection. *PLoS One* **6**, e22043 (2011).
49. M. J. Losman, T. M. Fasy, K. E. Novick, M. Monestier, Monoclonal autoantibodies to subnucleosomes from a MRL/Mp(-)+/+ mouse. Oligoclonality of the antibody response and recognition of a determinant composed of histones H2A, H2B, and DNA. *J Immunol* **148**, 1561-1569 (1992).
50. D. Boucher, C. Duclos, J. B. Denault, General in vitro caspase assay procedures. *Methods Mol Biol* **1133**, 3-39 (2014).

Acknowledgments: We thank Dr Vishva Dixit (Genentech) for GSDMD reagents, Dr Lin Luo for 3C protease, and Prof Arturo Zychlinsky for advice and useful discussions. **Funding**: This work was supported by the National Health and Medical Research Council of Australia (Project Grants 1064945 and 1122240 to KS, Senior Research Fellowship 1107914 to MJS, Career Development Fellowship 1141131 to KS) and the Australian Research Council (Future Fellowship FT130100361 to KS). DB was supported by a University of Queensland Postdoctoral Fellowship. P.B. is supported by a grant from the ERC (ERC-2017-CoG - 770988 - InflamCellDeath). Imaging was performed in the Australian Cancer Research Foundation-funded IMB Cancer Biology Imaging Facility. **Author contributions**: K.W.C., M.M. and D.B. designed and performed experiments, and analyzed data. J.B.vP. performed immunoblots. G.S. designed and performed experiments with human neutrophils. D.R. performed immunofluorescence on tissue sections. N.C. assisted with microscopy analysis. P.B. and M.J.S provided reagents and expert advice. K.W.C. and K.S. designed the study and wrote the manuscript with input from all authors. K.S. supervised the study. **Competing interests**: A/Prof Schroder is a co-inventor on patent applications for NLRP3 inhibitors which have been licensed to Inflazome Ltd, a company headquartered in Dublin, Ireland. Inflazome is developing drugs that target the NLRP3 inflammasome to address unmet clinical needs in inflammatory disease. The authors have no further conflicts of interest to declare.

Figure captions

Fig. 1. **Activated caspase-11 but not caspase-1 triggers neutrophil cell death. (A-D)** Neutrophils were primed with 100 ng/ml LPS for 4 h before stimulation with *Salmonella* Typhimurium (MOI 25, log phase) or nigericin (5 μM) for the indicated times: **(A, B)** caspase-1 (cleaved p20, or full length p46) in cell supernatants (Sup.) or cell lysates (Lys.) were measured by immunoblot. **(C-D)** lactate dehydrogenase (LDH) release was quantified to monitor cell lysis. **(E-K)** Neutrophils were primed with 1 μg/ml Pam3CSK4 for 4 h and transfected without (mock) or with ultrapure LPS (10 μg/ml) for 4 h. LDH release **(E,F,H)**, GSDMD cleavage to p30 **(G)** or IL-1β secretion **(I-K)** was monitored. **(L)** Neutrophils were primed with 1 μg/ml Pam3CSK4 for 4 h and transfected without (mock) or with ultrapure LPS (10 μg/ml) for 4 h, with and without KCl supplementation to the medium immediately before cell transfection. IL-1β release was quantified. Immunoblots are representative of data from at least three biological replicates. Graphs are mean + SEM from data pooled from three (K), four (H, L), six (I), seven (E) six to eight (F, J), or eight (C, D) biological replicates. Data were analyzed for normality using the Shapiro-Wilk normality test. Statistical analyses were performed using parametric t-tests (two-sided) for normally distributed data sets, and nonparametric Mann-Whitney t-tests (two-sided) for data sets with non-normal distributions. Data were considered significant when $p \leq 0.05$ (*), 0.01 (**), 0.001(***), or 0.0001(****).

Fig. 2. Neutrophils express limited caspase-1, and GSDMD is more efficiently cleaved by caspase-11 than caspase-1. (A) Macrophages (M) and neutrophils (N) were exposed to 100 ng/ml LPS or 1 μg/ml Pam3CSK4 for 4 h and cell extracts were analyzed by immunoblot for expression of inflammasome pathway components. **(B)** Cytosolic lysates of HEK293T expressing GSDMD-V5 or pro-IL-1β-V5 were incubated with recombinant caspase-1 or -11 for 30 min at 37°C, and substrate cleavage was assessed by anti-V5 immunoblot. **(C)** Neutrophils were primed with 1 μg/ml Pam3CSK4 for 4 h and transfected without agonist (mock) or with ultrapure LPS (10 μg/ml) or flagellin (1 μg/ml) for 4 h. Cell lysates and supernatants were

harvested and pooled for immunoblot analysis of GSDMD cleavage to p30. Blots are cropped from the same film. All data are representative of at least three biological replicates (A-C).

Fig. 3. LPS-activated caspase-11 induces NETosis via GSDMD. (A-D) Neutrophils were primed (1 μg/ml Pam3CSK4 for 4 h) and then transfected with either 10 μg/ml ultrapure LPS or 1 μg/ml flagellin for 4 h. Cells were stained for DNA (DAPI), myeloperoxidase (MPO) and citrullinated histone H3 (H3Cit). NETosis was examined by deconvolution immunofluorescence microscopy **(A-D)**. Images shown are representative of data from at least three biological replicates. **(C)** Microscopy images were blinded and quantified for NETosis, where cells with delobulated nuclei or diffuse/spread DNA were counted as cells undergoing NETosis. **(D)** Microscopy images were quantified using ImageJ for the percentage of cells that are positive for citrullinated histone H3. Graphs show mean + SEM of data from three biological replicates (C-D). Data were analyzed for normality (Shapiro-Wilk normality test) and significance (parametric two-sided t-test, $p \leq 0.001$***, or 0.0001****).

Fig. 4. The coordinated functions of GSDMD and caspase-11 drive early and late NETosis. (A) Murine neutrophils were primed (1 μg/ml Pam3CSK4 for 4 h) and then transfected without (mock) or with 10 μg/ml ultrapure LPS for 4 h. NETosis was examined by deconvolution immunofluorescence microscopy, and the percentage of cells undergoing early versus late NETosis was scored by blind counting for cells with delobulated nuclei or diffuse DNA (early) versus spread extracellular DNA (late). Data are mean +SEM of three biological replicates. Data were analyzed for normality (Shapiro-Wilk normality test) and significance (parametric two-sided t-test, $p \leq 0.01$**, or 0.0001****). **(B)** Murine neutrophils were primed (1 μg/ml Pam3CSK4 for 4 h) and then transfected without (mock) or with 10 μg/ml ultrapure LPS for 4 h. Cells were then fractionated to give cytosolic versus nuclear extracts, which were then analyzed by immunoblot. Data are representative of three biological replicates. **(C,D)** Nuclei of murine neutrophils were incubated for 15 mins with recombinant full length GSDMD, with or without recombinant caspase-11 to enable GSDMD cleavage to p30. Image analysis of **(C)** SYTOX uptake assessed permeabilization of the nuclear membrane, and **(D)** SYTOX volume assessed chromatin decondensation. Data are mean + SEM of $n>890$ cells, representative of at least 3

biological replicates. Statistical analyses were performed using nonparametric Mann-Whitney t-tests (two-sided; $p \leq 0.0001$****). **(E)** Nuclear extracts were prepared from murine neutrophils, and incubated with 100 nM recombinant caspase-11 for up to 2 h. Histone H3 cleavage was assessed by immunoblot, and quantified by densitometry using ImageJ. Data are representative of three biological replicates.

Fig. 5. A cytosolic Gram-negative bacterium induces NETosis of human neutrophils. Human neutrophils were primed for 2 h with 1 μg/ml Pam3CSK4 and then infected with *Citrobacter rodentium* in the presence and absence of the caspase-1/4 inhibitor, VX765 (50 μM). **(A)** NETosis for cells infected at MOI 25 was measured as SYTOX uptake over a 3 h time course. Data are mean ± SEM of infections of neutrophils from six healthy donors ($p \leq 0.0001$****, 2-way ANOVA). **(B)** NETosis was imaged by confocal microscopy, staining for myeloperoxidase (MPO) and extracellular chromatin relative to the DAPI DNA stain.

Fig. 6. Neutrophil infection with cytosolic bacteria triggers caspase-11/GSDMD-driven NETosis and *in vivo* host defense. (A-C) Neutrophils were primed for 4 h with 1 μg/ml Pam3CSK4 and then challenged with *Salmonella* Typhimurium *ΔsifA* (MOI 50, stationary phase) for 4 h, and NETosis was examined by deconvolution immunofluorescence microscopy. **(A)** Microscopy images, representative of three biological replicates. Microscopy images were quantified for **(B)** NETosis, and **(C)** the percentage of cells that were positive for citrullinated histone H3. Data are mean + SEM of three biological replicates. **(D)** Microscopy images were also quantified for the percentage of cells infected (mean + SEM of 18 fields of view from three biological replicates) and the number of bacteria per infected cell (>100 infected cells per genotype from three biological replicates). **(E)** WT, *Casp11*$^{-/-}$ and *Gsdmd*$^{-/-}$ mice were challenged with stationary phase *Salmonella* Typhimurium *ΔsifA* (1×10^5 CFU i.p.), with and without *in vivo* 150 U DNase I application at 4 h post-infection. Bacterial burden in the spleen was quantified at 24 h p.i. Data are geometric mean and individual values of five individual mice per treatment group. Data were analyzed for normality using the Shapiro-Wilk normality test. Statistical analyses were performed using two-sided parametric t-test (B, C, D upper) or

nonparametric Mann-Whitney t-test (D lower, E). Data were considered significant when $p \leq 0.05$*, 0.01**, 0.001***, or 0.0001****).

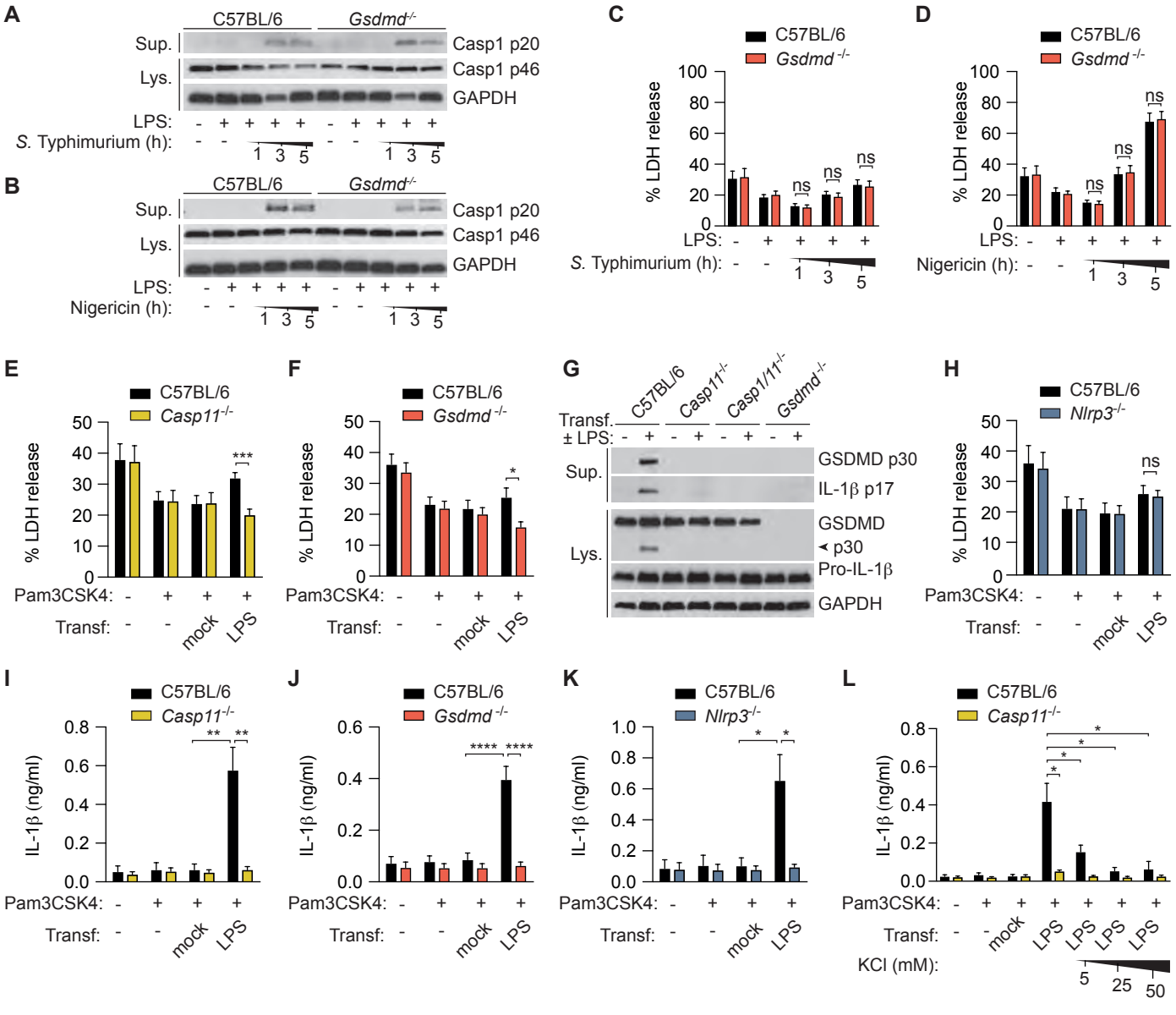
A
C57BL/6
Gsdmd-/-
Sup.
Lys.
Casp1 p20
Casp1 p46
GAPDH
LPS:
S. Typhimurium (h):
1 3 5
B
Nigericin (h):
C
% LDH release
ns
D
E
Casp11-/-
***
Pam3CSK4:
Transf:
mock
LPS
F
*
G
Casp1/11-/-
Transf.
± LPS:
GSDMD p30
IL-1β p17
GSDMD
p30
Pro-IL-1β
H
Nlrp3-/-
I
IL-1β (ng/ml)
**
J
****
K
L
KCl (mM):
5
25
50

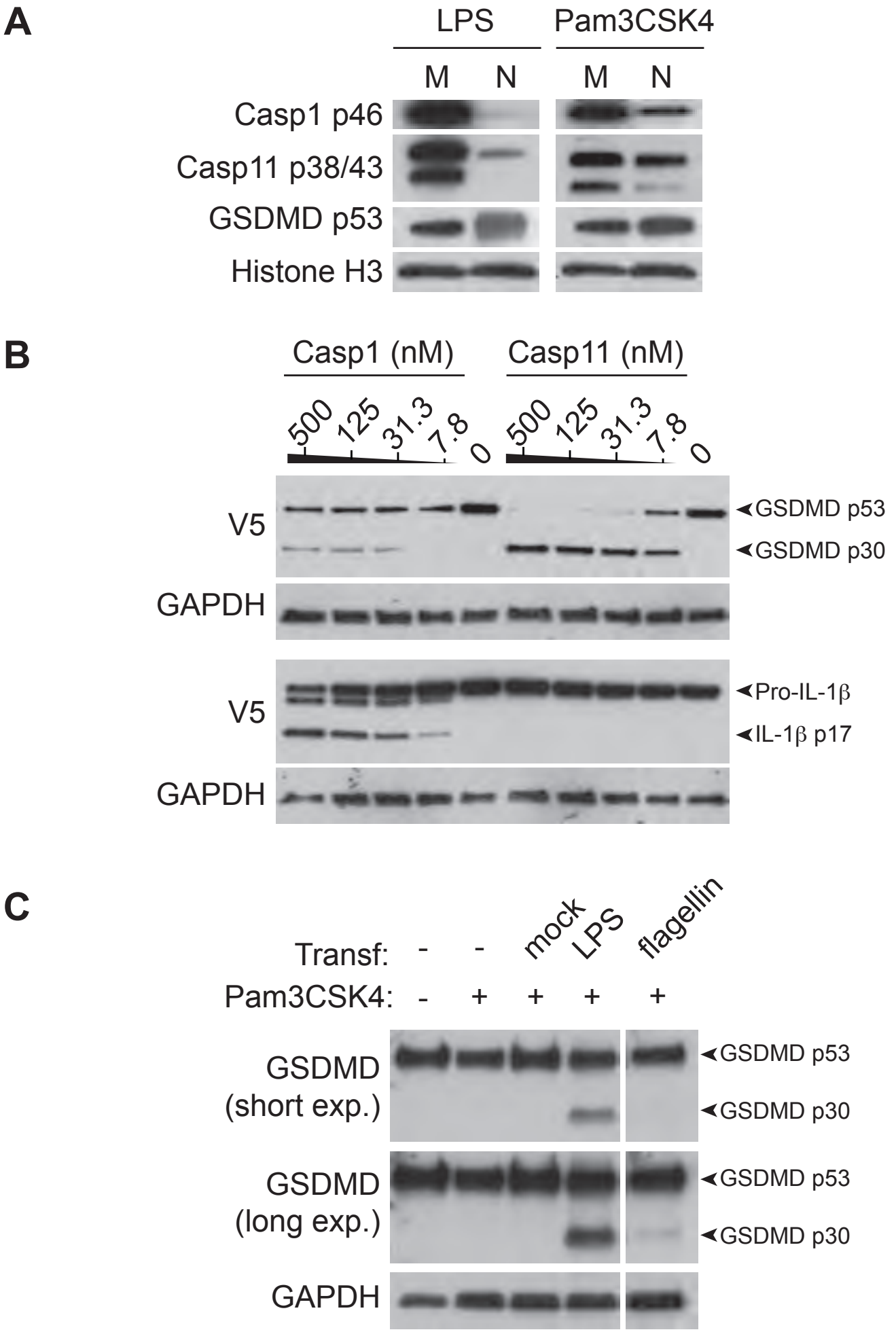
A
LPS
Pam3CSK4
M
N
M
N
Casp1 p46
Casp11 p38/43
GSDMD p53
Histone H3
B
Casp1 (nM)
Casp11 (nM)
500
125
31.3
7.8
0
500
125
31.3
7.8
0
V5
GSDMD p53
GSDMD p30
GAPDH
V5
Pro-IL-1β
IL-1β p17
GAPDH
C
Transf:
-
-
mock
LPS
flagellin
Pam3CSK4:
-
+
+
+
+
GSDMD
(short exp.)
GSDMD p53
GSDMD p30
GSDMD
(long exp.)
GSDMD p53
GSDMD p30
GAPDH

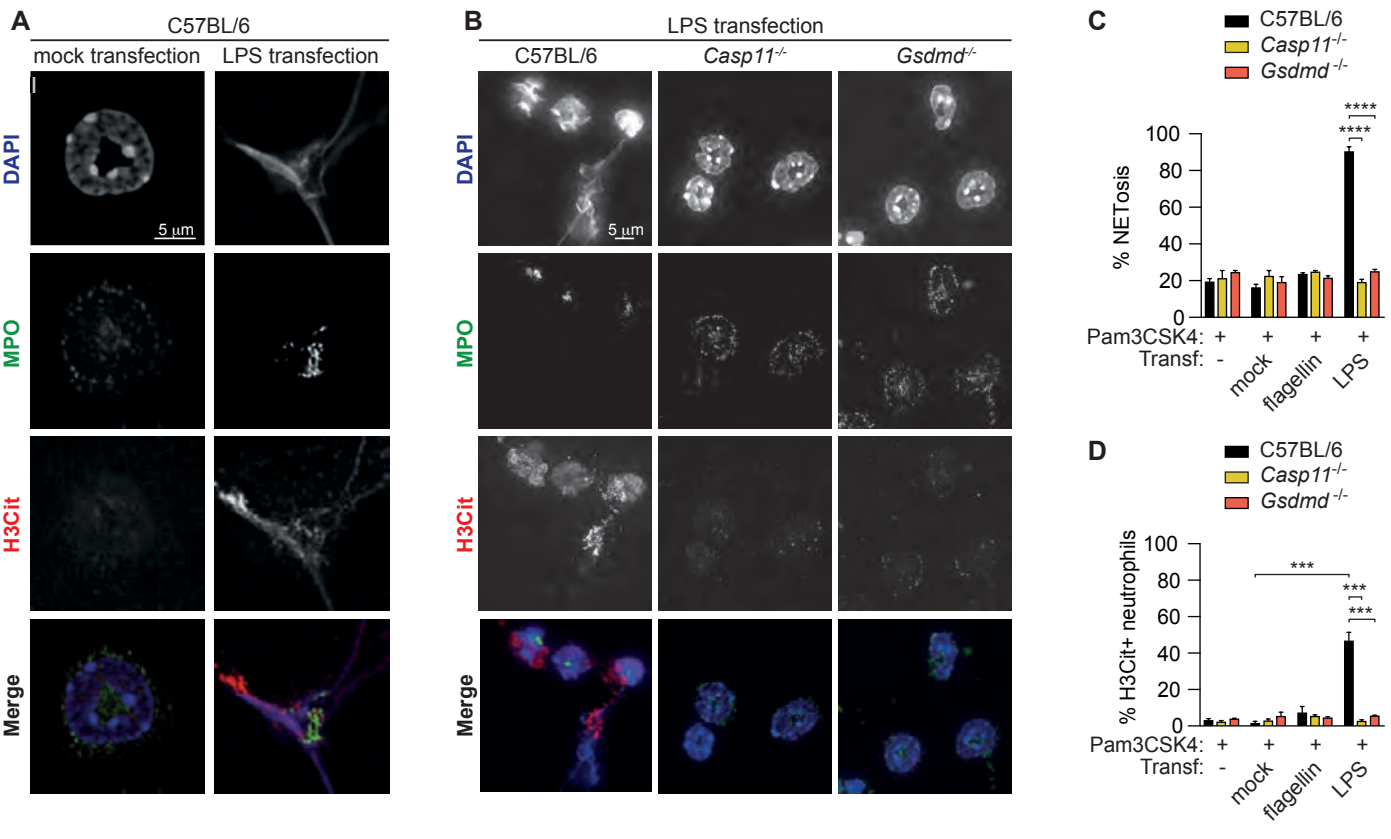
A
C57BL/6
mock transfection
LPS transfection
DAPI
MPO
H3Cit
Merge
5 μm
B
LPS transfection
C57BL/6
Casp11-/-
Gsdmd-/-
C
C57BL/6
Casp11-/-
Gsdmd-/-
% NETosis
Pam3CSK4:
Transf:
mock
flagellin
LPS
D
% H3Cit+ neutrophils

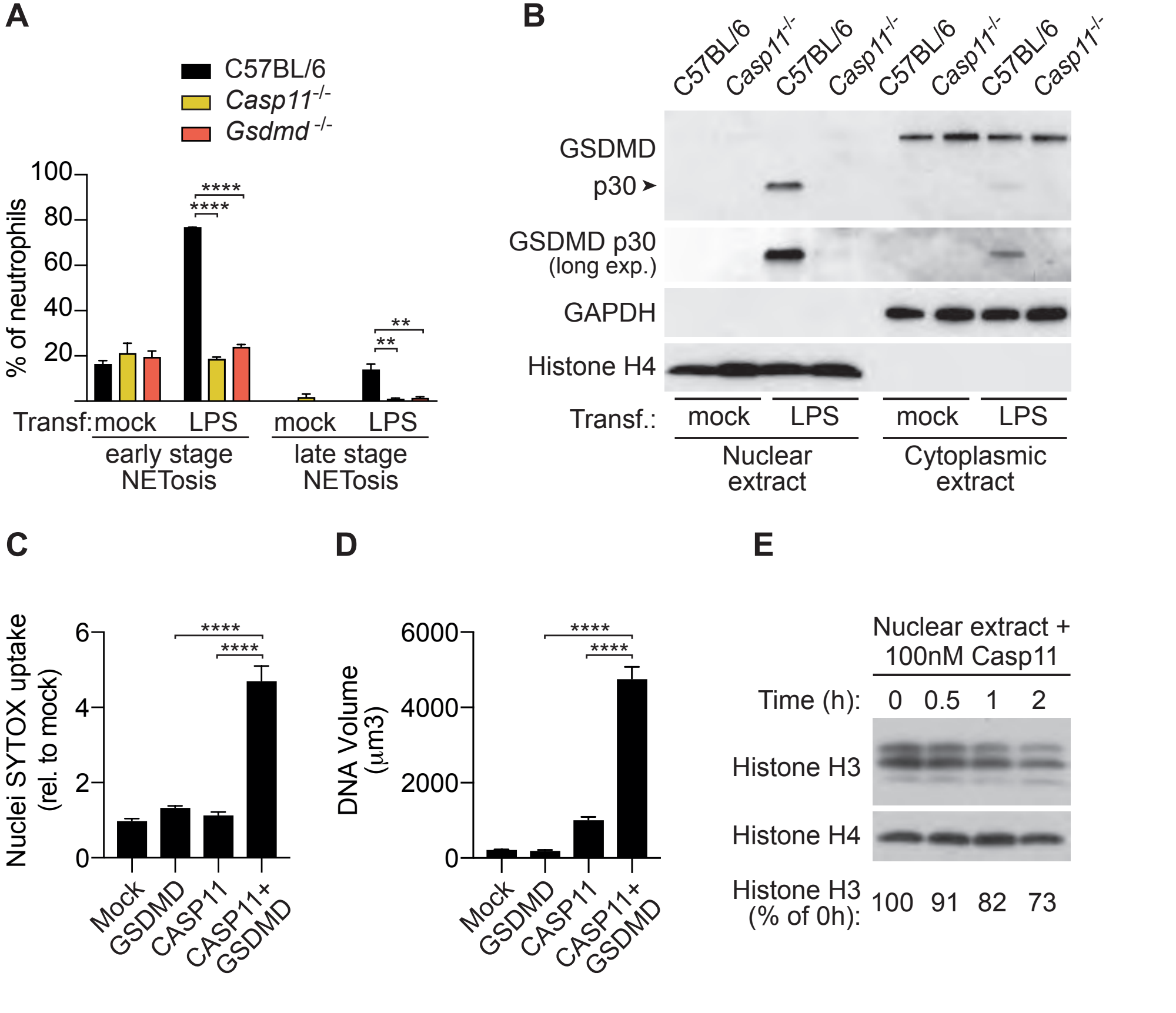
A
C57BL/6
Casp11-/-
Gsdmd-/-
% of neutrophils
100
80
60
40
20
****
****
**
**
Transf:
mock
LPS
mock
LPS
early stage NETosis
late stage NETosis
B
C57BL/6
Casp11-/-
C57BL/6
Casp11-/-
C57BL/6
Casp11-/-
C57BL/6
Casp11-/-
GSDMD
p30
GSDMD p30 (long exp.)
GAPDH
Histone H4
Transf.:
mock
LPS
mock
LPS
Nuclear extract
Cytoplasmic extract
C
Nuclei SYTOX uptake (rel. to mock)
6
4
2
0
****
****
Mock
GSDMD
CASP11
CASP11+ GSDMD
D
DNA Volume (µm3)
6000
4000
2000
0
****
****
Mock
GSDMD
CASP11
CASP11+ GSDMD
E
Nuclear extract + 100nM Casp11
Time (h):
0
0.5
1
2
Histone H3
Histone H4
Histone H3 (% of 0h):
100
91
82
73

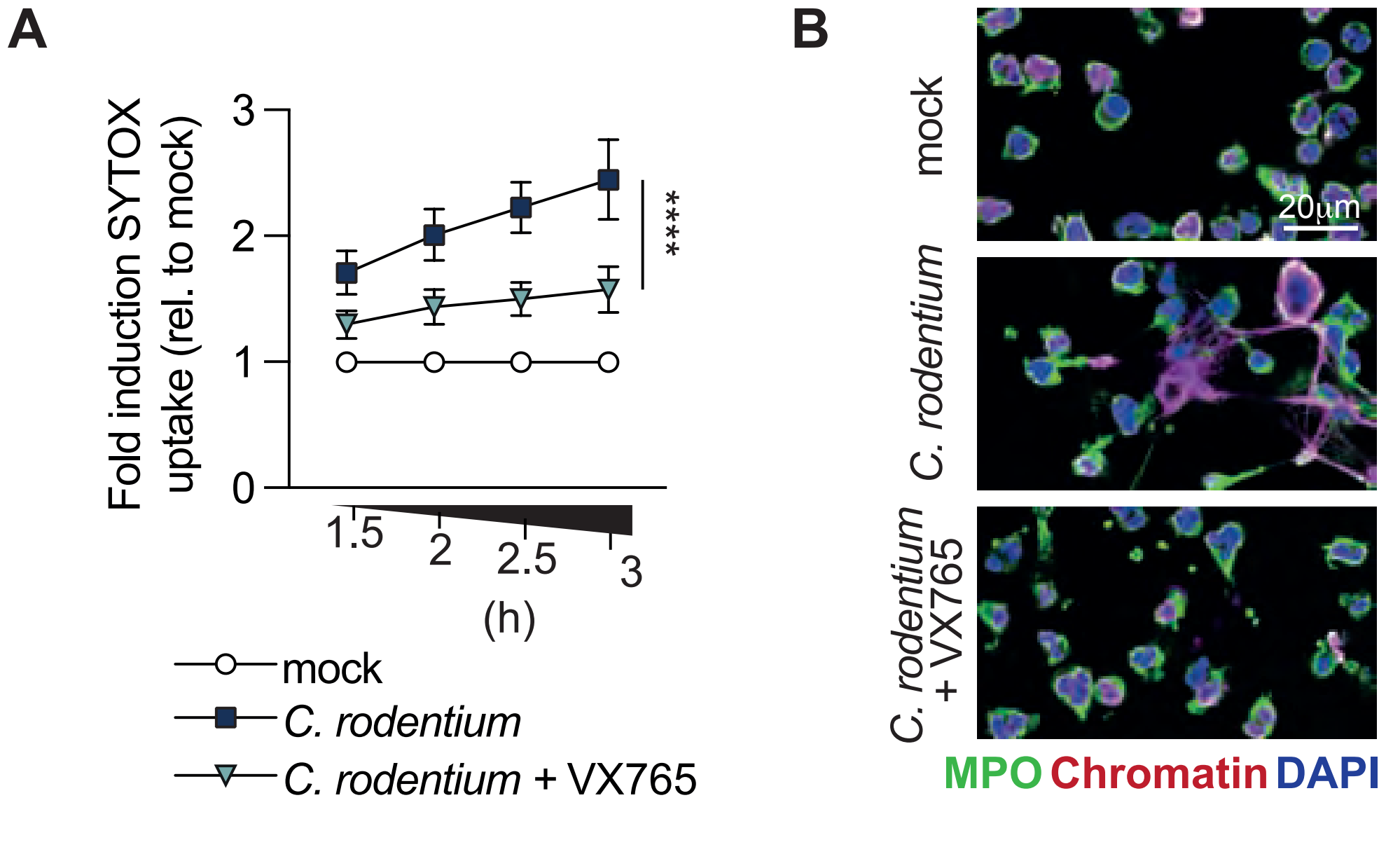
A
Fold induction SYTOX uptake (rel. to mock)
3
2
1
0
****
1.5
2
2.5
3
(h)
mock
C. rodentium
C. rodentium + VX765
B
mock
C. rodentium
C. rodentium + VX765
20µm
MPO Chromatin DAPI

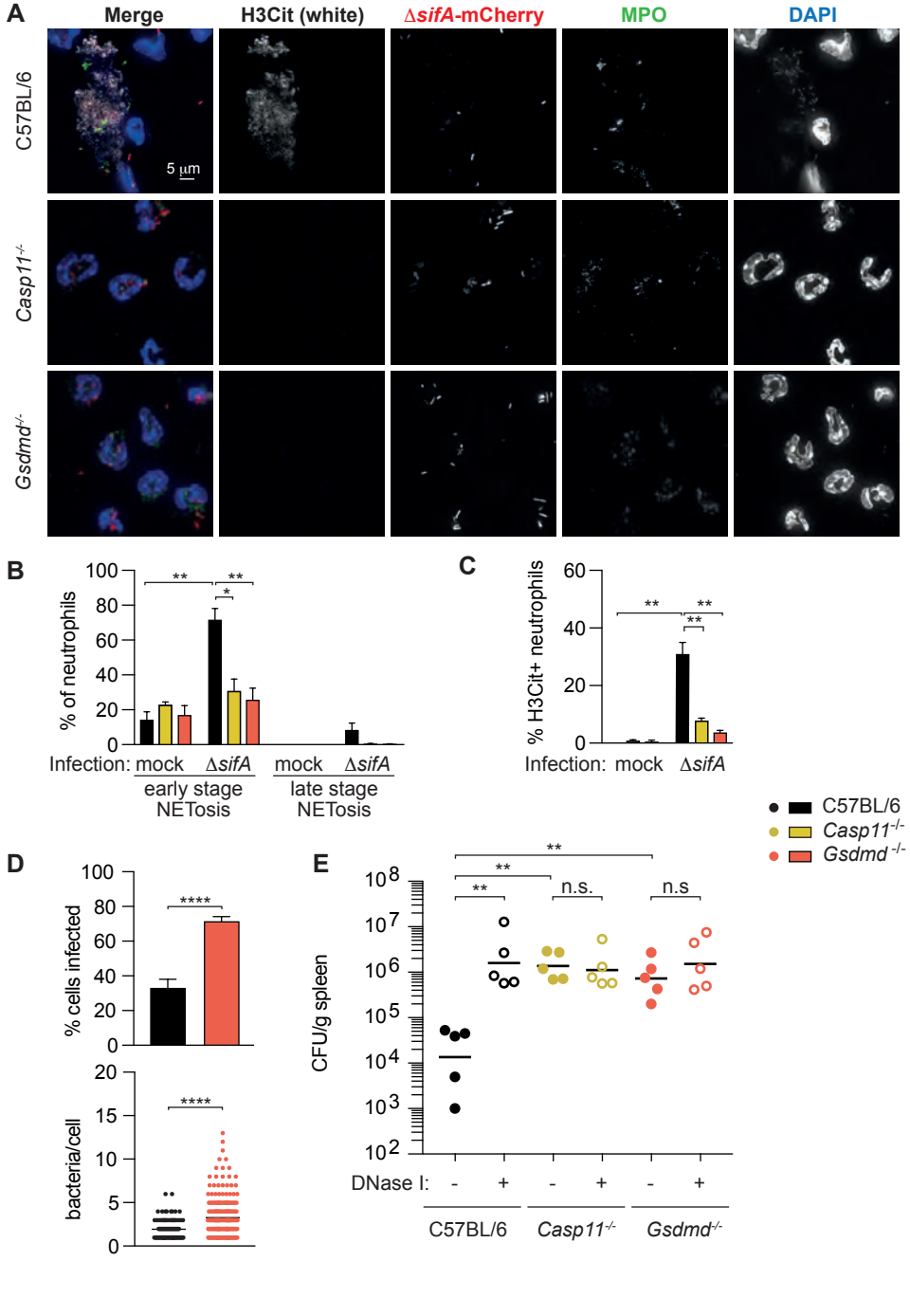
A
Merge
H3Cit (white)
ΔsifA-mCherry
MPO
DAPI
C57BL/6
Casp11-/-
Gsdmd-/-
5 µm
B
% of neutrophils
Infection: mock ΔsifA mock ΔsifA
early stage NETosis
late stage NETosis
C
% H3Cit+ neutrophils
Infection: mock ΔsifA
C57BL/6
Casp11-/-
Gsdmd-/-
D
% cells infected
bacteria/cell
E
CFU/g spleen
n.s.
DNase I: - + - + - +
C57BL/6
Casp11-/-
Gsdmd-/-

ScienceImmunology

Submitted Manuscript: Confidential template updated: July 5 2016

Supplementary materials

The non-canonical inflammasome provides host defense via gasdermin D-dependent neutrophil extracellular traps

Authors: Kaiwen W. Chen[1,2*], Mercedes Monteleone[1*], Dave Boucher[1*], Gabriel Sollberger[3], Divya Ramnath[1], Nicholas D. Condon[1], Jessica B. von Pein[1], Petr Broz[2], Matthew J. Sweet[1], Kate Schroder[1]†

Affiliations:

[1]Institute for Molecular Bioscience (IMB), and IMB Centre for Inflammation and Disease Research, The University of Queensland, St Lucia Brisbane 4072, Australia.

[2]Department of Biochemistry, University of Lausanne, CH-1066 Epalinges, Switzerland.

[3]Max Planck Institute for Infection Biology, Department of Cellular Microbiology, Charitéplatz 1, Berlin

*These authors contributed equally

†Corresponding author: Dr. Kate Schroder, Institute for Molecular Bioscience (IMB), and IMB Centre for Inflammation and Disease Research, The University of Queensland, St Lucia 4072, Australia. Tel: +61 7 3346 2058, Fax: +61 7 3346 2101, E-mail: K.Schroder@imb.uq.edu.au

One Sentence Summary: Neutrophils defend against cytosolic bacteria by extruding neutrophil extracellular traps via the pore-forming protein, gasdermin D.

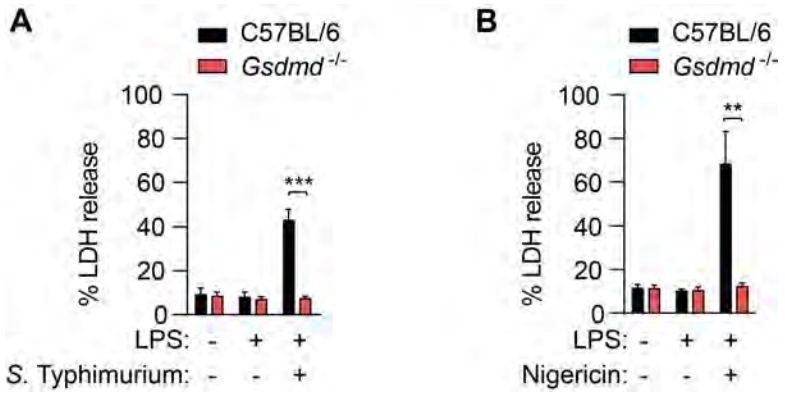

Fig. S1. GSDMD mediates rapid macrophage pyroptosis. Macrophages were primed for 4 h with 100 ng/ml LPS before stimulation for 1 h with **(A)** *Salmonella* Typhimurium (MOI 10, log phase) or **(B)** nigericin (5 μM). LDH release was measured as an indicator of cell death. Data are mean + SEM of four biological replicates. Statistical analyses were performed using parametric t-tests (two-sided; $p \leq 0.01$**, 0.001***) after confirming that data were normally distributed (Shapiro-Wilk normality test).

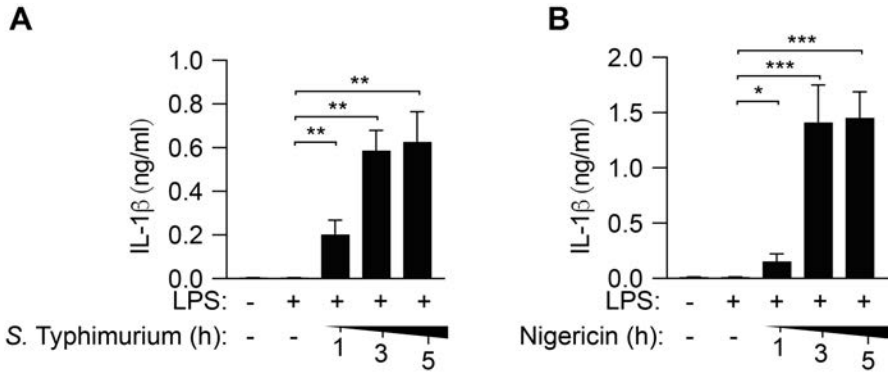

Fig. S2. *Salmonella* Typhimurium and nigericin induce IL-1β secretion from WT neutrophils. Neutrophils were primed with 100 ng/ml LPS for 4 h before stimulation with (A) *Salmonella* Typhimurium (MOI 25 log phase) or **(B)** nigericin (5 μM). Released IL-1β was quantified over time. Data are mean + SEM of six (A) or seven (B) biological replicates. Statistical analyses were performed using nonparametric Mann-Whitney t-tests (two-sided; $p \leq 0.05$*, 0.01**, 0.001***, or 0.0001****).

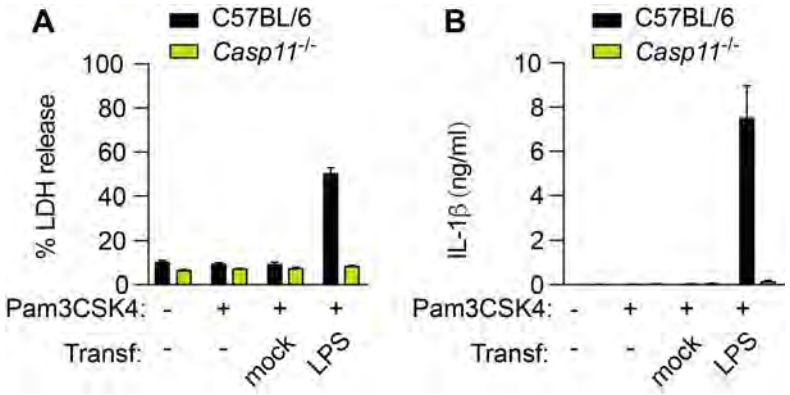

Fig. S3. Cytosolic LPS triggers caspase-11-dependent cell death and IL-1β production from macrophages. Bone marrow-derived macrophages were primed with 1 μg/ml Pam3CSK4 for 4 h and then transfected with ultrapure LPS (2 μg/ml) for 4 h. Release of **(A)** LDH and **(B)** IL-1β was quantified. Data are mean + SD of three technical replicates, and are representative of at least three biological replicates.

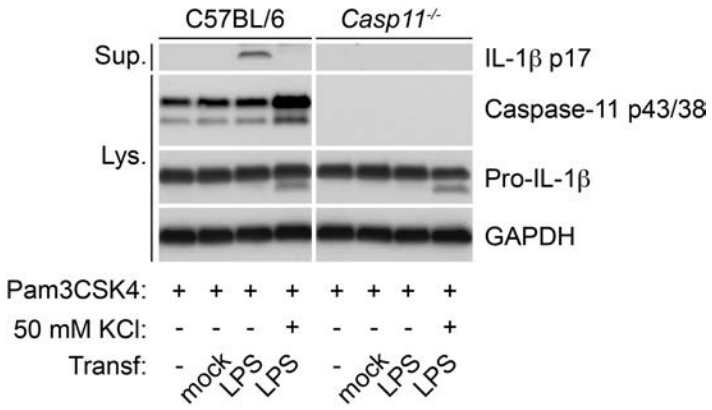

Fig. S4. Extracellular potassium blocks non-canonical NLRP3 activation and resultant release of mature IL-1β. Neutrophils were primed with 1 μg/ml Pam3CSK4 for 4 h and then transfected with ultrapure LPS (10 μg/ml), in the presence or absence of high extracellular potassium added to the cell culture medium immediately before transfection. Cell lysates and supernatants were analyzed by immunoblot 4 h later. Blots are cropped from the same film. Data are representative of four biological replicates.

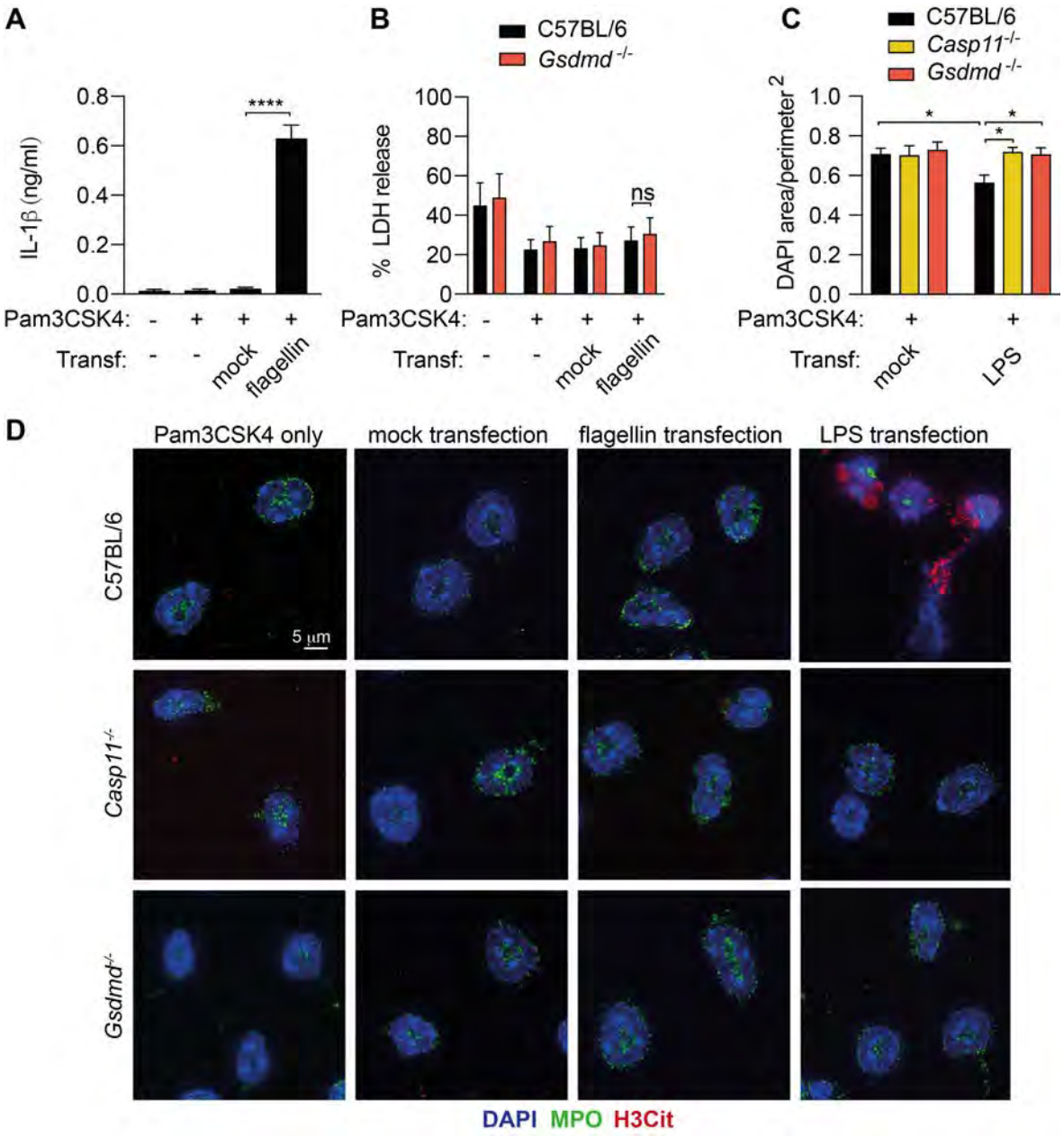

Fig. S5. Cytosolic LPS but not mock or flagellin transfection triggers GSDMD-dependent cell death. (A,B) Neutrophils were primed with 1 μg/ml Pam3CSK4 for 4 h before transfection with flagellin (1 μg/ml) for 4 h. IL-1β release from WT neutrophils, and LDH release from WT versus *Gsdmd*-deficient neutrophils was measured. Data are mean + SEM of three (B) or five (A) biological replicates. Statistical analyses were performed using parametric t-tests (two-sided; $p \leq 0.0001$***) after confirming that data were normally distributed (Shapiro-Wilk normality test). **(C,D)** Neutrophils were primed (1 μg/ml Pam3CSK4 for 4 h) and then transfected (mock, 10 μg/ml ultrapure LPS, 1 μg/ml flagellin) for 4 h: **(C)** LPS-induced nuclear changes (DAPI area/perimeter^2) were quantified using ImageJ (mean + SEM of n=5-30 cells; $p \leq 0.05$* nonparametric two-sided Mann-Whitney t-test); **(D)** NETosis was examined by deconvolution immunofluorescence microscopy. These images show the control samples for Fig. 3B, and are representative of data from at least three biological replicates.

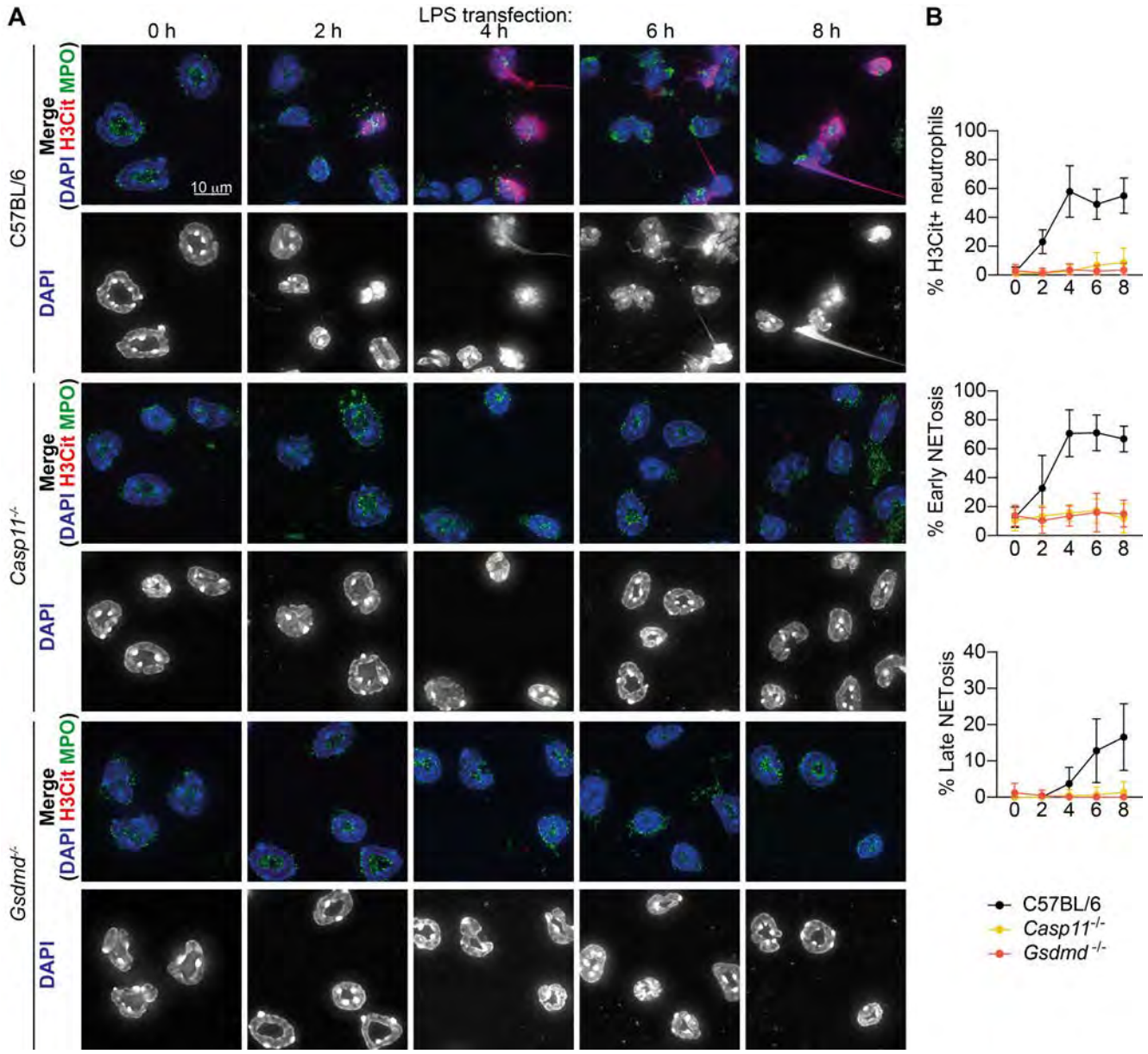

Fig. S6. Time course analysis profiles the kinetics of caspase-11/GSDMD-induced NETosis. Neutrophils were primed (1 µg/ml Pam3CSK4 for 4 h) and then transfected with 10 µg/ml ultrapure LPS for 0-8 h. Deconvolution immunofluorescence microscopy for DNA (DAPI), MPO and citrullinated histone H3 assessed neutrophil NETosis and histone citrullination, as for Fig. 3: **(A)** Images are representative of two biological replicates. **(B)** Microscopy images were quantified using ImageJ for the percentage of cells that are positive for citrullinated histone H3 (upper), and blinded images were and quantified for NETosis (middle, lower), where cells with delobulated nuclei or diffuse DNA were counted as cells undergoing early NETosis, while cells with extruded DNA were counted as cells undergoing late NETosis. Graphs are mean +SD of 10-11 fields of view from two biological replicates.

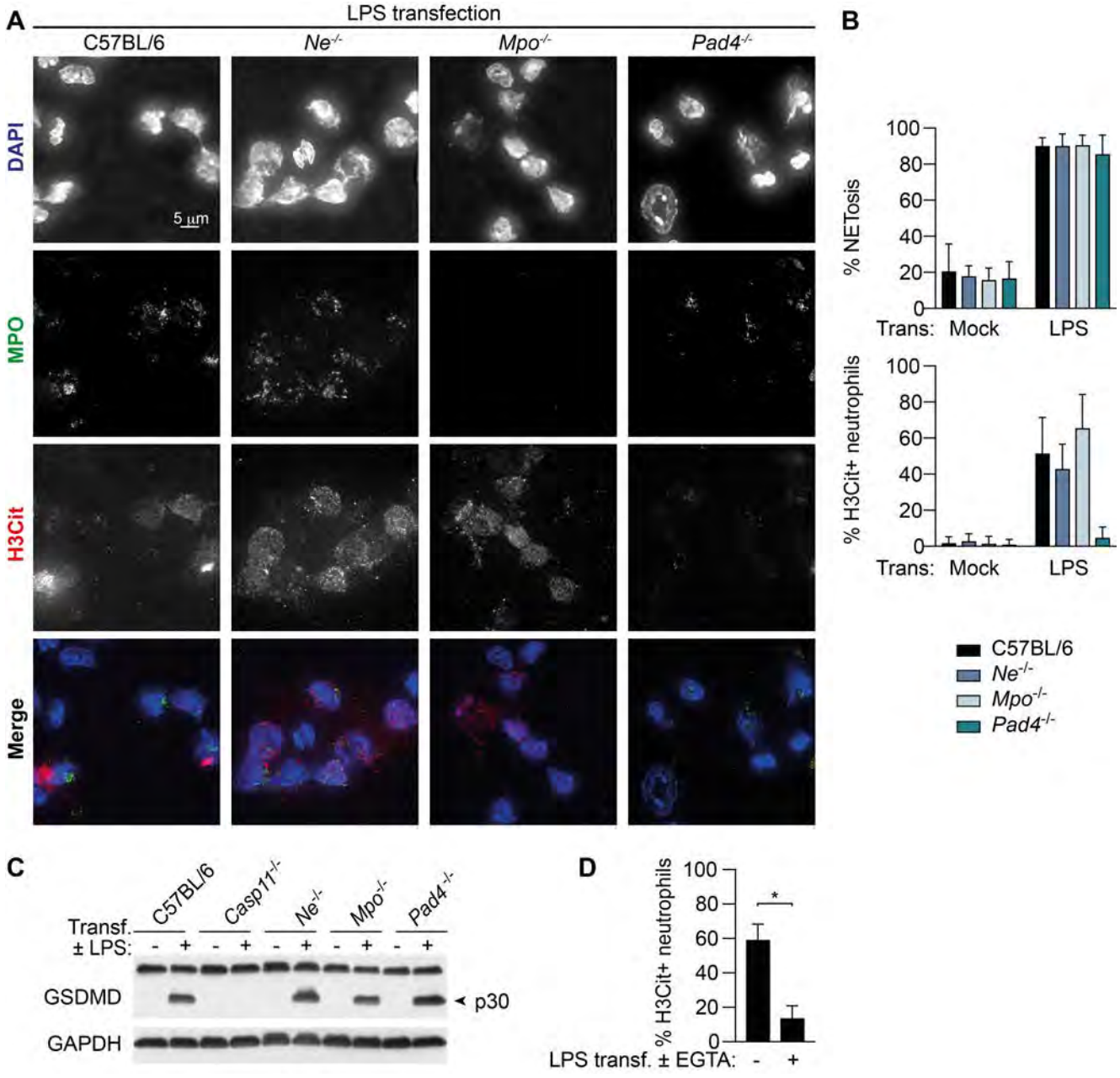

Fig. S7. NE, MPO, and PAD4 are dispensable for GSDMD cleavage and caspase-11-driven NETosis. (A-D) Neutrophils were primed (1 µg/ml Pam3CSK4 for 4 h) and then transfected with 10 µg/ml ultrapure LPS for 4 h, with or without the addition of 2.5 mM EGTA 30 min prior to LPS transfection. **(A-B, D)** Deconvolution immunofluorescence microscopy for DNA (DAPI), MPO and citrullinated histone H3 assessed neutrophil NETosis and histone citrullination, as for Fig. 3. Graphs are **(B)** mean +SD of 10-12 fields of view from two biological replicates, or **(D)** mean +SEM of three biological replicates ($p \leq 0.05$* parametric t-test following the Shapiro-Wilk normality test). **(C)** Whole cell extracts were prepared by precipitating supernatants and resuspending them in lysates. GSDMD cleavage was assessed by immunoblot, representative of two biological replicates.

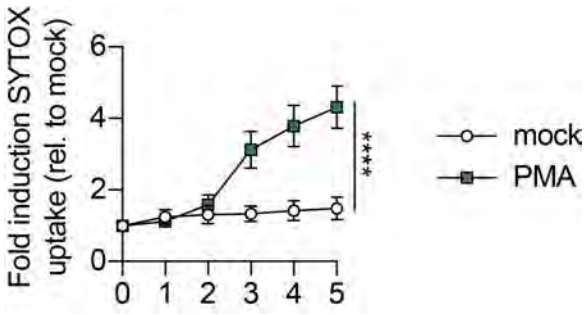

Fig. S8. PMA induces NETosis of human neutrophils. Human neutrophils were exposed to 100 nM PMA. Cells were analyzed using the membrane-impermeable nucleic acid dye, SYTOX green, over 5 h. Data are mean + SEM of four independent blood donors ($p \leq 0.0001$****, 2-way ANOVA).

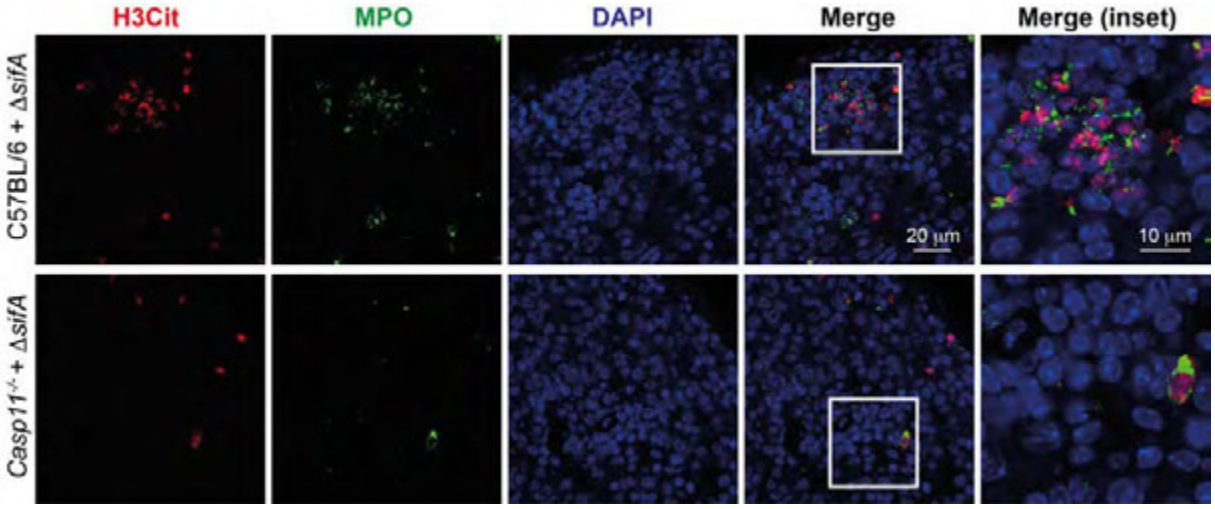

Fig. S9. Cytosolic bacteria triggers caspase-11-dependent NETs *in vivo*. WT and *Casp11*$^{-/-}$ mice were challenged with stationary phase *Salmonella* Typhimurium *ΔsifA* (1 x 10^5 CFU i.p.). Spleen sections were examined by immunofluorescence at 48 h post-infection. Images are representative of data from four mice per condition.

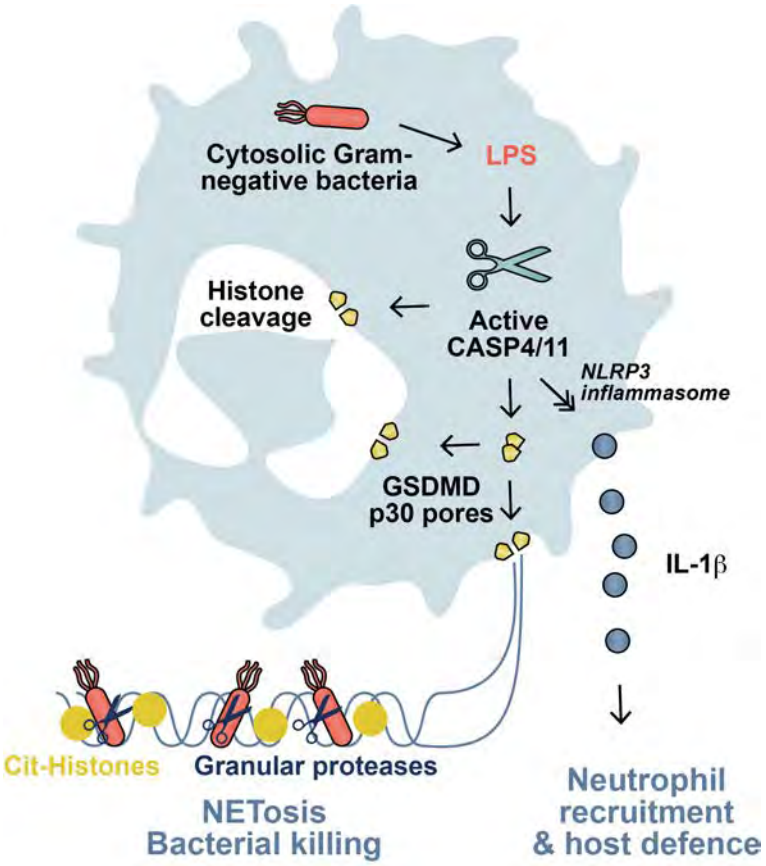

Fig. S10. Model for LPS-driven NETosis via GSDMD during cytosolic infection. The LPS of cytosolic Gram-negative bacteria binds to, and activates, caspase-4/11 within the non-canonical inflammasome complex, leading to GSDMD cleavage, pore formation and perforation of the nuclear and plasma membranes. GSDMD-driven nuclear permeabilization allows caspase-11 to access chromatin, leading to histone clipping and inactivation and DNA expansion. GSDMD-dependent plasma membrane rupture then allows the neutrophil to expel its decondensed chromatin. During caspase-11-driven NETosis, PAD4 becomes activated, likely via calcium influx through GSDMD pores, and PAD4 citrullinates histone H3. GSDMD-mediated membrane permeabilization also triggers activation of the NLRP3 inflammasome and resultant IL-1β production. While both PAD4-dependent histone H3 citrullination and NLRP3-dependent IL-1β production accompany NETosis, they are not required for NETosis. Caspase-4/11-driven NETosis also proceeds independently of neutrophil elastase and myeloperoxidase. In inducing the death of neutrophils infected with cytosolic Gram-negative bacteria, caspase-4/11-driven NETosis prevents cytosolic infection, and extruded NETs prevent bacterial dissemination *in vivo*.